DOI: 10.1534/genetics.109.106880

Pharmacogenetic Analysis Reveals a Post-Developmental Role for Rac GTPases in *Caenorhabditis elegans* GABAergic Neurotransmission

Cody J. Locke,*[,1,2] Bwarenaba B. Kautu,*[,1] Kalen P. Berry,* S. Kyle Lee,* Kim A. Caldwell*[,†,3] and Guy A. Caldwell*[,†,3]

**Department of Biological Sciences, The University of Alabama, Tuscaloosa, Alabama 35487 and †Departments of Neurobiology and Neurology and Center for Neurodegeneration and Experimental Therapeutics, University of Alabama, Birmingham, Alabama 35294*

Manuscript received July 1, 2009
Accepted for publication September 17, 2009

ABSTRACT

The nerve-cell cytoskeleton is essential for the regulation of intrinsic neuronal activity. For example, neuronal migration defects are associated with microtubule regulators, such as LIS1 and dynein, as well as with actin regulators, including Rac GTPases and integrins, and have been thought to underlie epileptic seizures in patients with cortical malformations. However, it is plausible that post-developmental functions of specific cytoskeletal regulators contribute to the more transient nature of aberrant neuronal activity and could be masked by developmental anomalies. Accordingly, our previous results have illuminated functional roles, distinct from developmental contributions, for *Caenorhabditis elegans* orthologs of LIS1 and dynein in GABAergic synaptic vesicle transport. Here, we report that *C. elegans* with function-altering mutations in canonical Rac GTPase-signaling-pathway members demonstrated a robust behavioral response to a $GABA_A$ receptor antagonist, pentylenetetrazole. Rac mutants also exhibited hypersensitivity to an acetylcholinesterase inhibitor, aldicarb, uncovering deficiencies in inhibitory neurotransmission. RNA interference targeting Rac hypomorphs revealed synergistic interactions between the dynein motor complex and some, but not all, members of Rac-signaling pathways. These genetic interactions are consistent with putative Rac-dependent regulation of actin and microtubule networks and suggest that some cytoskeletal regulators cooperate to uniquely govern neuronal synchrony through dynein-mediated GABAergic vesicle transport in *C. elegans*.

EPILEPSY affects 1–2% of the world population and is associated with imbalances between excitatory and inhibitory neurotransmission in the brain (Locke *et al.* 2009). In particular, interneurons expressing gamma-aminobutyric acid (GABA), the principal inhibitory neurotransmitter in the human brain, are essential for normal neuronal synchronization and maintenance of a seizure threshold in humans (Cossette *et al.* 2002), rodents (Delorey *et al.* 1998), and zebrafish (Baraban *et al.* 2005). A failure of the brain to properly regulate neuronal synchrony can result from ion channel defects (Xu and Clancy 2008), neuropeptide depletion (Brill *et al.* 2006), brain malformations (Patel *et al.* 2004), interneuron loss (Cobos *et al.* 2005), and/or synaptic vesicle recycling failure (Di Paolo *et al.* 2002), all of which may be caused by disrupting the nerve-cell cytoskeleton. Therefore, further exploration of putative links between cytoskeletal components and neurotransmission may accelerate development of novel therapeutics for epilepsy.

Epilepsy associated with cytoskeletal dysfunction often has a developmental basis (Di Cunto *et al.* 2000; Wenzel *et al.* 2001; Keays *et al.* 2007). For example, mutations in *LIS1*, a dynein motor complex regulator, lead to classical lissencephaly, which is characterized by neuronal migration defects, a lack of convolutions in the brain, mental retardation, and epileptic seizures (Lo Nigro *et al.* 1997). Yet, observations that lissencephaly-associated seizures worsen after neuronal migration ceases, while *LIS1* expression persists, imply that *LIS1* also acts in the adult brain (Cardoso *et al.* 2002).

We previously reported that *C. elegans* with a predicted null mutation (*t1550*) in *lis-1*, the worm ortholog of human *LIS1*, exhibited synaptic vesicle misaccumulations, but not neuronal migration or axon-pathfinding defects, in GABAergic motor neurons. We also observed anterior "epileptic-like" convulsions, which were intense, frequent, and repetitive, with *lis-1*(*t1550*) homozygotes in the presence of pentylenetetrazole (PTZ; Williams *et al.* 2004), an epileptogenic $GABA_A$ receptor antagonist (Huang *et al.* 2001; Fernandez *et al.* 2007). PTZ sensitivity was also increased in heterozygous *lis-1(t1550)* mutants following RNA interference (RNAi)

Supporting information is available online at http://www.genetics.org/cgi/content/full/genetics.109.106880/DC1.

[1]These authors contributed equally to this work.

[2]*Present address:* Neuroscience Program, University of California, San Francisco, CA 94158.

[3]*Corresponding authors:* Department of Biological Sciences, The University of Alabama, Box 870344, Tuscaloosa, AL 35487-0344.
E-mail: gcaldwel@bama.ua.edu and kcaldwel@bama.ua.edu

against worm orthologs of associated cortical malformation genes, such as *cdk-5* and *nud-2*, which are known to interact with *LIS1* and the dynein motor complex. Depletion of these gene products was coincident with dynein-mediated synaptic vesicle transport defects, not with architectural defects, in GABAergic motor neurons (Locke *et al.* 2006).

Plausible functional interactions among LIS-1, dynein, and Rac GTPases (Rehberg *et al.* 2005; Kholmanskikh *et al.* 2006) have not been explored in an intact adult nervous system. *C. elegans* is ideal for characterizing these interactions due to the availability of weak and strong Rac pathway mutants (Lundquist *et al.* 2001; Poinat *et al.* 2002; Lucanic *et al.* 2006), a comprehensive RNAi library (Kamath *et al.* 2003), and GFP-based neuronal markers. Here, we combine these tools with pharmacological modifiers of neuronal activity and establish an experimental paradigm that reveals a novel regulatory pathway. This pathway is composed of integrins at the plasma membrane that signal through Racs to dynein-associated proteins, which function to coordinate synaptic vesicle transport in larval and adult GABAergic motor neurons.

MATERIALS AND METHODS

Worm strains and maintenance: *C. elegans* were maintained via standard procedures (Brenner 1974). The following strains were used: Bristol N2, *avr-14(ad1302) avr-15(ad1051) glc-1(pk54)*, *cat-2(e1112)*, *ced-2(n1994)*, *ced-5(n1812)*, *ced-10(n1993)*, *ced-10(n3246)*, *dgk-1(nu62)*, *dhc-1(js121)/hT2[bli-4(e937) let-?(q782) qIs48]; jsIs37*, *eat-4(ky5)*, *egl-8(md1971)*, *egl-10(md176)*, *goa-1(sa734)*, *ina-1(gm39)*, *ina-1(gm144)*, *lis-1(t1550) unc-32(e189)/qC1 dpy-19(e1259) glp-1(q339); him-3(e1147)*, *mig-2(gm103)*, *mig-2(mu28)*, *mig-15(rh80)*, *mig-15(rh148)*, *mig-15(rh326)*, *rab-3(y251)*, *swan-1(ok267)*, *tom-1(ok188)*, *tph-1(mg280)*, *unc-5(e53)*, *unc-17(e245)*, *unc-25(e156)*, *unc-26(e1196)*, *unc-30(e191)*, *unc-32(e189)*, *unc-34(e315)*, *unc-34(e566)*, *unc-40(n324)*, *unc-49(e407)*, *unc-51(e396)*, *unc-73(e936)*, *unc-73(ev802)*, *unc-73(rh40)*, *unc-115(ky275)*, $P_{unc-115}$::*mig-2(G16V)*, $P_{unc-115}$::*rac-2(G12V)*, *juIs1* (P_{unc-25}::SNB-1::GFP), and *oxIs12* (P_{unc-47}::GFP).

Behavioral and pharmacological assays: Convulsion assays were performed, as previously described (Williams *et al.* 2004; Locke *et al.* 2008). Concentrations of PTZ (Sigma) employed are indicated in the text. Aldicarb-induced paralysis assays also were performed, as described (Nonet *et al.* 1998), by transferring young adult hermaphrodites to NGM plates with 0.5 mM aldicarb (Supelco). Worms were observed in 30-min intervals for a period of 3 hr.

For thrashing assays, 1-day-old adult worms were washed clean of bacteria with M9, transferred to 7.5-ml NGM plates with 2 ml M9, and allowed to recover for 2 min. Movies of worms thrashing were captured in real-time with a Q Imaging Retiga Exi digital video camera at 25 frames/sec. Movies were saved onto an Intel Pentium computer using ImageJ (National Institutes of Health, Bethesda, MD) and scored at a reduced frame rate for accuracy. A thrash was defined as a change in direction at the worm mid-body.

Other methods used: Details of the rescue of *ina-1* are available in the supporting information, File S1. Descriptions of the genetic crosses and fluorescence microscopy analyses used to observe possible alterations in GABAergic D-type motor neuron architecture and/or synaptic vesicle distribution are provided in File S1. RNAi by bacterial feeding was performed, as described (Locke *et al.* 2006), with slight modifications (see File S1).

Statistical analysis: Statistical analyses of all data sets, except for those obtained from thrashing assays, were performed using Fisher's exact test (http://www.langsrud.com/fisher.htm). Results given are two-tail *P*-values, which were found by comparing two appropriate data sets for specified comparisons. Statistical analyses of data sets from thrashing assays were performed using Student's *t*-test. Data are shown as mean ± SD and were deemed significant, if $P < 0.05$, for both statistical tests.

RESULTS

PTZ induces anterior convulsions in Rac GTPase-signaling-pathway mutants: We previously demonstrated that worms lacking LIS-1 exhibit PTZ-induced anterior convulsions. We also found these behavioral responses to be associated with loss of GABA because systemic GABA mutants (*i.e.*, *unc-25* and *unc-47*) demonstrated similar responses to PTZ (Williams *et al.* 2004). Moreover, we previously used PTZ to reveal genetic interactions among *lis-1* and other microtubule-dependent cortical malformation genes (Locke *et al.* 2006). Intriguingly, LIS-1 orthologs have also been shown to interact with Rac1 in Dictyostelium and mammals to shape the actin cytoskeleton (Kholmanskikh *et al.* 2003; Rehberg *et al.* 2005). These findings suggest an evolutionarily conserved role for LIS-1 and actin regulators, whose impact on intrinsic neuronal activity is undefined.

To determine if *C. elegans* Racs modulate neuronal synchrony, we exposed loss- and gain-of-function Rac mutants to PTZ. The products of worm *ced-10*, *mig-2*, and *rac-2* genes act redundantly in multiple developmental processes, including axon pathfinding in GABAergic D-type motor neurons (Lundquist *et al.* 2001). The Rac gain-of-function (gf) mutant allele, *ced-10(n3246)*, confers axon-pathfinding defects similar to those resulting from multiple Rac loss-of-function (lf) mutations and is predicted to interfere with a common guanine nucleotide exchange factor (GEF) of redundant Racs (Shakir *et al.* 2006). A second Rac gf mutant allele, *mig-2(gm103)*, has been shown to perturb axon pathfinding (Zipkin *et al.* 1997), vulval cell migration (Kishore and Sundaram 2002), and male tail development (Dalpé *et al.* 2004) in a manner consistent with cross-inhibition of redundant Rac pathways (Zipkin *et al.* 1997; Lundquist *et al.* 2001). We found that, like a strong systemic GABA mutant (Figure 1A; Figure S1; File S2), both *ced-10(n3246)* (Figure 2; File S3) and *mig-2(gm103)* (Figure S1; File S4) mutants had anterior PTZ-induced convulsions (Figure 1A). The frequency and intensity of convulsions positively correlated with PTZ concentration, similar to *lis-1(t1550)* and systemic GABA mutant responses to PTZ (Williams *et al.* 2004). Neither of the Rac lf mutants, *ced-10(n1993)* and *mig-2(mu28)*, had altered PTZ sensitivity, compared to *C. elegans* N2, wild-type, worms

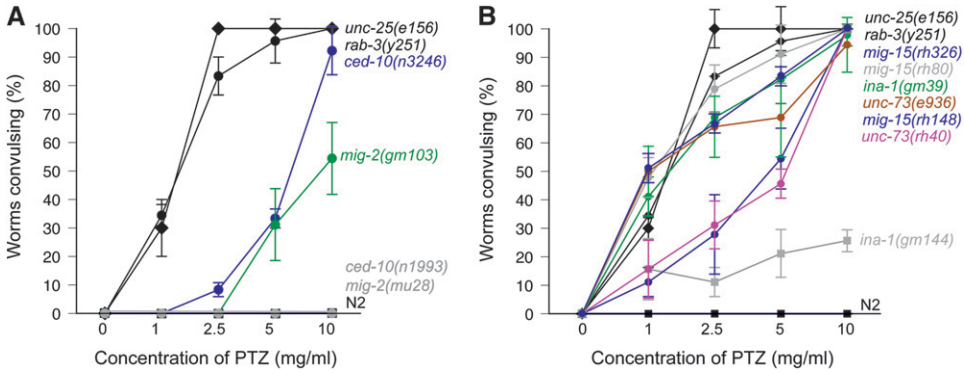

FIGURE 1.—Rac GTPase and canonical Rac regulator mutant anterior convulsions are commensurate with increasing concentrations of PTZ. (A and B) The response level (the percentage of young adult worms convulsing per total sample size; $n = 30$ for each of three independent experiments) of various *C. elegans* strains is depicted for each PTZ concentration, ranging from 0 to 10 mg/ml. N2 wild-type worms (black squares) did not exhibit anterior convulsions at any tested concentration of PTZ. Conversely, representative GABA (black diamonds) and general synaptic transmission (black circles) mutants did exhibit PTZ-induced anterior convulsions. (A) Rac gain-of-function (blue and green circles), but not loss-of-function mutants (collectively shown by gray circles), demonstrated PTZ-induced anterior convulsions. (B) Rac regulator mutants also displayed PTZ-induced anterior convulsions. Although both *unc-73* Rac GEF mutants were hypersensitive to PTZ, the weakest mutant tested, *e936* (brown circles), was more sensitive to PTZ than a stronger *unc-73* Rac GEF mutant, *rh40* (purple circles). The strongest *mig-15* mutant tested, *rh326* (blue circles), was more sensitive to PTZ than a weaker *mig-15* mutant, *rh148* (blue circles), but was not significantly different from a *mig-15* mutant, *rh80* (gray circles), of intermediate strength. Hypomorphic alpha integrin (*ina-1*) mutants, *gm39* (green circles) and *gm144* (gray squares), were hypersensitive to PTZ. Of these two mutants, *gm39*, thought to be the weakest, exhibited the greatest sensitivity, as 97.8 ± 3.8% convulsed on 10 mg/ml PTZ, whereas 25.6 ± 3.8% of *gm144* worms convulsed at the same concentration. Each data point represents mean ± SD.

(Figure 1A). A putative *rac-2* lf allele, *ok326*, did not alter PTZ sensitivity (Table 1). These data suggest that CED-10, MIG-2, and perhaps RAC-2 play redundant roles in controlling *C. elegans* inhibitory GABA transmission.

Rac GTPases are known to function in a variety of neurobiological processes, including neurite branching and extension, axon pathfinding, and synapse formation. Furthermore, Rac GTPases are regulated by a number of other proteins, which are not simply limited to GEFs and GTPase-activating proteins (GAPs) (DE CURTIS 2008). To determine which, if any, known *C. elegans* Rac regulators modulate neuronal synchrony, we exposed an array of Rac regulator mutants to PTZ. A Rac GTPase-signaling pathway, which is governed by interactions between *C. elegans* orthologs of integrins and Nck-interacting kinase (NIK), mediates GABAergic D-type motor neuron axon pathfinding (POINAT *et al.* 2002). Consistent with a role for these Rac regulators in GABAergic neurotransmission, multiple *ina-1* (α-integrin) and *mig-15* (NIK) hypomorphs demonstrated anterior epileptic-like convulsions in response to PTZ (Figure 1B; Figure 2; Figure S1; File S5; File S6). The percentages of *mig-15* mutants with anterior convulsions (Figure 1B) were roughly coincident with the strengths of mutant alleles, where *rh326* > *rh80* > *rh148* (SHAKIR *et al.* 2006). Yet, the frequencies of *rh326* and *rh80* mutant convulsions were not significantly different from each other (Figure 1B). Surprisingly, *ina-1(gm39)* mutants had higher percentages of PTZ-induced convulsions at all concentrations than *ina-1(gm144)* mutants, which are predicted from cell migration defects to be weaker (BAUM and GARRIGA 1997) (Figure 1B). Perhaps *gm39* disrupts the binding of a different number and/or class of ligands than *gm144* disrupts

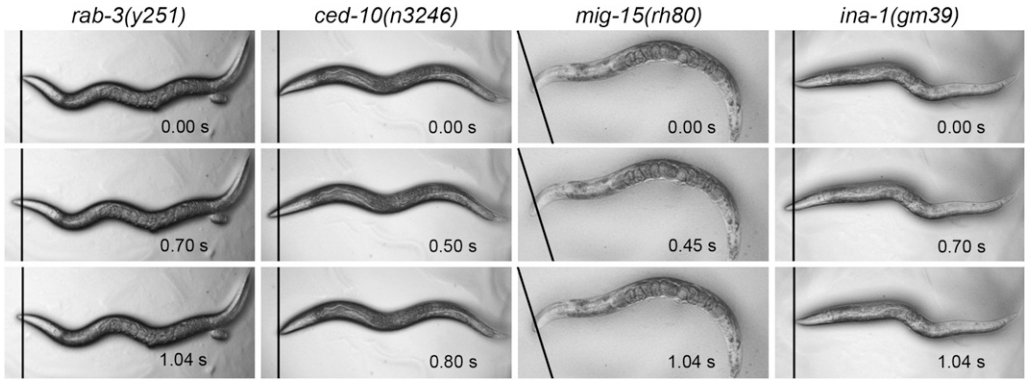

FIGURE 2.—Still-frame images demonstrating *C. elegans* mutant strains with anterior convulsions in response to 10 mg/ml PTZ. The still images are representative frames from movies (25 frames/sec), which are available in the supporting information. The black lines represent stationary reference points for visualization of anterior movements in relation to time ("s" indicates seconds). Anterior is to the left in all images where lines are placed perpendicularly to the original position of each worm's nose. The convulsions of a general synaptic transmission mutant, *rab-3(y251)*, mimic those of a Rac gain-of-function mutant, *ced-10(n3246)*, and the Rac regulator mutants, *mig-15(rh80)* and *ina-1(gm39)*. Bar, 100 μm.

TABLE 1

***C. elegans* mutants of interest exhibiting no PTZ-induced anterior convulsions**

Gene name	Allele name	Protein identity	*C. elegans* neuronal function(s)	Reference
Rac GTPase signaling				
rac-2	*ok326*	One of three triply redundant Rac GTPases	Axon pathfinding; cell migration; cell corpse engulfment	Lundquist *et al.* (2001)
unc-73	*ev802*	Rho/Rac guanine nucleotide exchange factor	Axon pathfinding; cell migration; neurotransmitter release	Struckhoff and Lundquist (2003); Williams *et al.* (2007)
ced-2	*n1994*	Src homology 2- and 3-containing adaptor	Axon pathfinding; cell migration; cell corpse engulfment	Wu *et al.* (2002); Kinchen *et al.* (2005)
ced-5	*n1812*	Signaling protein, DOCK180, ortholog	Axon pathfinding; cell migration; cell corpse engulfment	Wu *et al.* (2002); Kinchen *et al.* (2005); Lundquist *et al.* (2001)
unc-115	*ky275*	Actin-binding protein, limatin, ortholog	Axon pathfinding	Struckhoff and Lundquist (2003)
swan-1	*ok267*	WD40 repeat-containing AN11-like protein	Negative regulation of Racs	Yang *et al.* (2006)
Netrin signaling				
unc-34	*e315*	Enabled/VASP ortholog	Axon pathfinding; cell migration	Gitai *et al.* (2003); Lucanic *et al.* (2006); Shakir *et al.* (2006)
unc-34	*e566*	Enabled/VASP ortholog	Axon pathfinding; cell migration	Gitai *et al.* (2003); Lucanic *et al.* (2006); Shakir *et al.* (2006)
unc-40	*n324*	Netrin receptor, DCC, ortholog	Axon pathfinding; cell migration	Gitai *et al.* (2003); Lucanic *et al.* (2006)
unc-5	*e53*	Netrin receptor	Axon pathfinding; cell migration	Gitai *et al.* (2003); Lucanic *et al.* (2006)
GABA transmission at body-wall muscles				
unc-30	*e191*	Homeodomain transcription factor	D-type motor neuron differentiation	Jin *et al.* (1994)
Non-GABA transmission				
unc-17	*e245*	Vesicular acetylcholine transporter	Acetylcholine transmission	Miller *et al.* (1996)
cat-2	*e1112*	Tyrosine hydroxylase	Dopamine transmission	Sulston *et al.* (1975)
eat-4	*ky5*	Vesicular glutamate transporter	Glutamate transmission	Rankin and Wicks (2000)
tph-1	*mg280*	Tryptophan hydroxylase	Serotonin transmission	Keane and Avery (2003)
General synaptic transmission				
tom-1	*ok188*	Tomosyn ortholog	Negative regulation of neurotransmitter release	McEwen *et al.* 2006

DCC, deleted in colorectal cancer.

(Baum and Garriga 1997). Future studies with candidate INA-1 ligands should assess this hypothesis.

We also observed PTZ-induced convulsions with a pair of *unc-73* mutants, which are deficient in UNC-73 GEF-dependent activation of the triply redundant Racs (Struckhoff and Lundquist 2003). The weaker *unc-73(e936)* mutants, which carry a splice donor mutation that disrupts all Rac GEF-containing isoforms of UNC-73, had higher percentages of PTZ-induced convulsions than stronger *unc-73(rh40)* mutants, which lack UNC-73 guanosine-5′-diphosphate to guanosine-5′-triphosphate exchange activity (Steven *et al.* 1998) (Figure 1B; Figure S1; File S7). This result could be due to disruption of GEF2 Rho GEF activity by *e936* (Steven *et al.* 1998). GEF2 Rho GEF activity may contribute to PTZ sensitivity, as it has been previously linked to normal synaptic transmission in *C. elegans* (Steven *et al.* 2005; Williams *et al.* 2007). Yet, GEF2 Rho GEF-deficient *unc-73(ev802)* mutants (Steven *et al.* 2005) did not exhibit altered PTZ sensitivities (Table 1), indicating that loss of GEF2 Rho GEF activity alone is not sufficient to allow for PTZ-induced convulsions.

We also did not observe altered PTZ sensitivities in *ced-2(n1994)* or *ced-5(n1812)* lf mutants (Table 1), which disrupt Rac-dependent cell corpse engulfment (Kinchen *et al.* 2005), cell migration, and axon pathfinding (Wu

TABLE 2

***C. elegans* Rac-signaling-pathway mutants with PTZ-induced anterior convulsions**

Gene name	Mutant allele(s)	Protein identity	Human homolog	BLAST *E*-value[a]
ced-10	*n3246*	One of three triply redundant Rac GTPases	*RAC1*	7.0*e*-87
mig-2	*gm103*	One of three triply redundant Rac GTPases	*RAC1*	1.7*e*-69
ina-1	*gm144*, *gm39*	α-Integrin subunit	*ITGA6*	8.2*e*-84
mig-15	*rh148*, *rh326*, *rh80*	Nck-interacting kinase	*MAP4K4*	1.2*e*-284
unc-73	*e936*, *rh40*	Rho/Rac guanine nucleotide exchange factor	*TRIO*	9.1*e*-237

[a] BLAST *E*-value obtained from WormBase (http://www.wormbase.org).

et al. 2002), suggesting that a different Rac-dependent mechanism underlies PTZ-induced convulsions. Likewise, we were unable to detect PTZ-induced convulsions with *unc-40(n324)* netrin receptor null mutants (Table 1), which are deficient in Rac-dependent GABAergic D-type motor neuron axon pathfinding (Lucanic *et al.* 2006) and non-GABAergic neuron axon pathfinding (Gitai *et al.* 2003). We also did not observe PTZ-induced convulsions with multiple lf mutants of *unc-34*, which has been shown to function in parallel to Rac mutants, downstream of UNC-40, in *C. elegans* axon pathfinding (Gitai *et al.* 2003; Lucanic *et al.* 2006; Shakir *et al.* 2006) or a second netrin receptor null mutant, *unc-5(e53)* (Lucanic *et al.* 2006; Table 1). Mutants lacking SWAN-1, which negatively regulates Rac mutants in neuronal and non-neuronal cells (Yang *et al.* 2006), or UNC-115, which positively regulates RAC-2, but not CED-10 or MIG-2, in GABAergic D-type motor neuron axon pathfinding (Struckhoff and Lundquist 2003), also did not have PTZ-induced convulsions (Table 1). These data suggest that UNC-73 activation of redundant Rac mutants, not Rho, lowers PTZ sensitivity in a manner that depends on integrins, not netrins. We have found that Rac-signaling mutants phenocopy *lis-1(t1550)* and systemic GABA mutants by exhibiting anterior convulsions on PTZ (Table 2). Yet, generalized synaptic transmission defects lower a threshold for PTZ-induced convulsions, as another general synaptic transmission mutant, *rab-3(y251)*, convulses on PTZ (Figure 1, A and B; Figure 2; File S8). Thus, we cannot resolve if this Rac pathway plays a GABA-specific role in worm neurons by PTZ.

The *C. elegans* inhibitory GABAergic nervous system is composed of 19 D-type motor neurons that innervate body-wall muscles and four nerve ring RME (ring motor) neurons that innervate head muscles (McIntire *et al.* 1993). Deficits in a single class of inhibitory GABAergic neurons could be sufficient for PTZ-induced convulsions. To address this possibility, we examined *unc-30(e191)* null mutants, which express wild-type levels of GABA in RME neurons but fail to express GABA in D-type motor neurons (Jin *et al.* 1994). We did not observe convulsions in these mutants with any PTZ concentration tested (Table 1), implying that RMEs may be chiefly responsible for this behavioral phenotype. Yet, these data do not rule out a contributory role for D-type motor neurons in convulsions.

GABA may not be the only source of inhibitory transmission at head muscles because *unc-49(e407)*-predicted null $GABA_A$ receptor mutants respond to PTZ in a dose-dependent manner (Williams *et al.* 2004). The *C. elegans* genome contains sequences for many other $GABA_A$ receptor homologs, including glutamate-gated chloride (GluCl) channels, which could function redundantly with *unc-49* (Schuske *et al.* 2004). In support of this argument, predicted null *unc-49* mutants have been shown to respond to a GABA agonist, muscimol, albeit less strongly than wild-type worms (McIntire *et al.* 1993). Likewise, predicted null *unc-49* GABA mutants also do not display RME neuron-mediated "loopy" foraging defects, unlike other GABA-deficient worms, further suggesting redundancy among $GABA_A$ receptor homologs (McIntire *et al.* 1993). To elucidate roles of other neurotransmitters in PTZ-induced convulsions, we assayed mutants systemically lacking acetylcholine [*unc-17(e245)*] (Miller *et al.* 1996), dopamine [*cat-2(e1112)*] (Sulston *et al.* 1975), glutamate [*eat-4(ky5)*] (Rankin and Wicks 2000), or serotonin [*tph-1(mg280)*] (Keane and Avery 2003) on PTZ. None of these mutants had PTZ-induced convulsions (Table 1). Yet, 28.9% of triple GluCl channel mutants [*avr-14(ad1302); avr-15(ad1051) glc-1(pk54)*], which lack inhibitory glutamate transmission at the nerve ring (Dent *et al.* 2000), displayed anterior convulsions in the presence of 10 mg/ml PTZ (File S9), whereas 100.0% of these mutants had anterior convulsions in the presence of 20 mg/ml PTZ. We did not observe convulsions in N2 worms at these concentrations of PTZ. These results may explain the failure of strong GABA mutants, such as *unc-25(e156)*, to spontaneously convulse (Williams *et al.* 2004). Indeed, *C. elegans* GluCl channels may also be perturbed by PTZ. Picrotoxin (PTX), a second epileptogenic $GABA_A$ receptor antagonist, has been shown to block invertebrate GluCl's (Etter *et al.* 1999). Since PTX and PTZ interact with overlapping domains of $GABA_A$ receptors (Huang *et al.* 2001), they may similarly block worm GluCl's. Yet, because the triple GluCl mutant convulsions are substantially less frequent and intense than convulsions of Rac-signaling mutants or systemic GABA mutants, it is likely that Rac-signaling

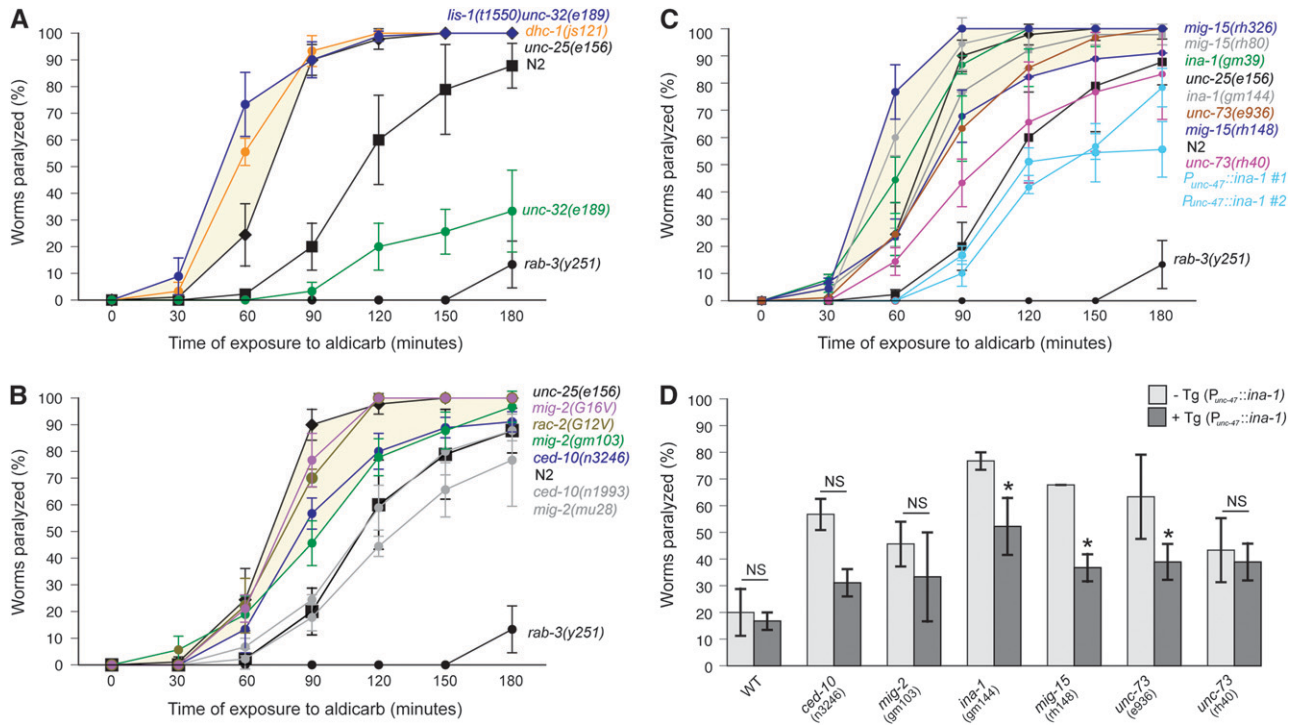

FIGURE 3.—Dynein motor complex and canonical Rac-signaling pathway mutants have increased neuromuscular excitability, as revealed by hypersensitivity to aldicarb. (A–C) The response level (the percentage of young adult worms paralyzed per total sample size; $n = 30$ for each of three independent experiments) of various *C. elegans* strains is depicted for each 30-min time point over a 3-hr exposure to 0.5 mM aldicarb. Paralysis of N2 wild-type worms (black squares) was commensurate with the time of aldicarb exposure. A representative GABA mutant (*unc-25*, black diamonds) was hypersensitive to aldicarb, whereas a general synaptic vesicle transport mutant (*rab-3*, black circles) was resistant to aldicarb when compared to wild type. (A) A hypomorphic *dhc-1* mutant, *js121* (orange circles), demonstrated hypersensitivity to aldicarb. Likewise, a predicted *lis-1* null mutant (blue circles) exhibited robust aldicarb hypersensitivity, despite also carrying a mutation (*unc-32*) that confers resistance to aldicarb in isolation (green circles). (B) Rac loss-of-function mutants (collectively shown by gray circles) exhibited wild-type aldicarb sensitivities. However, Rac gain-of-function mutants (blue and green circles) and transgenic worms, which express either constitutively active *mig-2(G16V)* (purple circles) or *rac-2(G12V)* (brown circles) under the control of the neuron-specific *unc-115* promoter ($P_{unc-115}$), were hypersensitive to aldicarb. (C) Rac regulator mutants also displayed hypersensitivity to aldicarb. A higher percentage of mutants with a weak Rac GEF allele, *unc-73(e936)* (brown circles), was paralyzed at 1 hr of aldicarb exposure, compared with mutants in a stronger Rac GEF allele, *unc-73(rh40)* (purple circles) at the same time. Conversely, significantly fewer mutants with the weakest *mig-15* allele, *rh148* (dark blue circles), were paralyzed after 1 hr of aldicarb exposure, compared to the percentage of mutants with the strongest *mig-15* allele, *rh326* (dark blue circles), or to the percentage of mutants with a *mig-15* allele of intermediate strength, *rh80* (gray circles). Likewise, there was a differential paralysis observed between *ina-1(gm39)* (green circles) and *ina-1(gm144)* (gray squares) mutants after 1 hr of aldicarb exposure. Notably, very few N2 wild-type worms were paralyzed after 1 hr of aldicarb exposure. All dynein motor complex, Rac gain-of-function, and regulator mutants were hypersensitive at 60 and 90 min. Two independently generated transgenic lines, which overexpress an *ina-1* cDNA transgene under the control of the GABAergic neuron-specific *unc-47* promoter (P_{unc-47}), were resistant to aldicarb (light blue circles). Each data point represents mean ± SD. Trends in sensitivity are shown in pale yellow. (D) The response level (the percentage of young adult worms paralyzed per total sample size; $n = 30$ for each of three independent experiments) of various *C. elegans* Rac-signaling mutants with (+) or without (−) an *ina-1* cDNA transgene (Tg) under the control of P_{unc-47} is depicted for 90 min of aldicarb exposure. Averaged results from two independently generated P_{unc-47}::*ina-1* transgenic lines are shown. GABAergic neuron overexpression of *ina-1* did not significantly affect aldicarb sensitivity of wild-type (WT) worms at this time point. Similarly, P_{unc-47}::*ina-1* failed to alter aldicarb sensitivity of either the Rac gain-of-function mutants *n3246* or *gm103* or the strongest Rac-deficient GEF mutant, *unc-73(rh40)*. Yet, GABAergic neuron overexpression of *ina-1* significantly reduced aldicarb hypersensitivity of weaker *ina-1(gm144)*, *mig-15(rh148)*, and *unc-73(e936)* mutants. Each data point represents mean ± SD.

mutants are GABA deficient. We hypothesize that loss of UNC-49 significantly lowers an intrinsic threshold, which PTZ overcomes by antagonizing other partially redundant $GABA_A$ receptor homologs on RME-innervated muscles. Future experiments, including electrophysiology, will be needed to better describe the roles of $GABA_A$ receptor homologs in *C. elegans* neurons.

LIS-1, dynein, and Rac-signaling-pathway mutants are hypersensitive to aldicarb: Excitatory acetylcholine (Ach) transmission and inhibitory GABA transmission antagonize each other at *C. elegans* body-wall neuromuscular junctions (NMJs) (RICHMOND and JORGENSEN 1999). Accordingly, *C. elegans* mutants with deficits in general synaptic transmission, such as *rab-3(y251)*, are resistant to paralysis from an acetylcholinesterase in-

hibitor, aldicarb (Figure 3, A–C; Nguyen *et al.* 1995; Miller *et al.* 1996). Conversely, *C. elegans* mutants with an inability to negatively regulate ACh transmission (Robatzek and Thomas 2000) or positively regulate inhibitory GABA transmission, such as *unc-25(e156)* (Figure 3, A–C; Jiang *et al.* 2005; Vashlishan *et al.* 2008), are hypersensitive to aldicarb. To better characterize synaptic transmission defects associated with *lis-1* and dynein mutations, we exposed a collection of mutants to aldicarb and monitored the time course of paralysis. The *lis-1(t1550)* lf mutant, which is genetically linked to *unc-32(e189)* and convulses on PTZ (Williams *et al.* 2004), was hypersensitive to aldicarb (Figure 3A). The *lis-1*-associated aldicarb hypersensitivity was substantial, considering that *unc-32(e189)* mutants were resistant to aldicarb (Figure 3A), as previously reported (Nguyen *et al.* 1995). Consistent with a role for the dynein motor complex in *lis-1*-associated aldicarb sensitivity, a hypomorphic *dhc-1* mutant allele, *js121*, also conferred hypersensitivity to aldicarb (Figure 3A). In support of our findings, another study has shown that RNAi against other members of the *C. elegans* dynein motor complex results in hypersensitivity to aldicarb (Vashlishan *et al.* 2008). These data suggest that LIS-1 and the dynein motor complex govern neuronal synchrony at worm NMJs by controlling ACh transmission.

To determine if a Rac GTPase-signaling pathway, such as LIS-1 and the dynein motor complex, participates in synaptic transmission at *C. elegans* NMJs, we exposed Rac and Rac regulator mutants to aldicarb. Consistent with functionally redundant roles for Racs in synaptic transmission, both *ced-10(n1993)* and *mig-2(mu28)* lf mutants demonstrated wild-type sensitivities to aldicarb (Figure 3B). Conversely, transgenic worms, expressing constitutively active *mig-2(G16V)* or *rac-2(G12V)* under the control of the neuron-specific *unc-115* promoter ($P_{unc\text{-}115}$) (Lucanic *et al.* 2006), were hypersensitive to aldicarb (Figure 3B). Similarly, the Rac gf mutants *ced-10(n3246)* and *mig-2(gm103)* were hypersensitive to aldicarb (Figure 3B), suggesting cross-inhibition of redundant Racs.

Hypomorphic *ina-1* and *mig-15* mutants, as well as Rac-deficient *unc-73* mutants, were also hypersensitive to aldicarb (Figure 3C). INA-1 is known to function upstream of Racs during axon pathfinding of GABAergic motor neurons (Poinat *et al.* 2002) and may also function upstream of Racs post-developmentally in synaptic transmission on the basis of our pharmacological results. To test if INA-1 contributes to aldicarb sensitivity through integrin and Rac-signaling pathways in GABAergic motor neurons, we used a GABA-specific *unc-47* promoter ($P_{unc\text{-}47}$) to drive the expression of *ina-1* in various genotypic backgrounds. Overexpression of *ina-1* in GABAergic neurons significantly decreased the aldicarb sensitivity of wild-type worms (Figure 3C). Overexpression of *ina-1* also partially rescued the aldicarb hypersensitivity of *ina-1(gm144)*, *mig-15(rh148)*, and *unc-73(e936)* hypomorphs (Figure 3D). Conversely, *ina-1* overexpression did not rescue the aldicarb hypersensitivity of the dominant Rac gf mutant or the strongest available Rac-deficient GEF mutant, *unc-73(rh40)* (Figure 3D), which is consistent with INA-1 functioning upstream of Racs in GABAergic motor neurons. Overexpression of *ina-1* in GABAergic neurons of the Rac gf mutants *n3246* and *gm103* may trend toward significance (Figure 3D) due to integrin-dependent modulation of parallel Rac pathways. These results suggest that a Rac-signaling pathway, dependent upon Trio, integrin, and NIK, could mediate sensitivity to aldicarb via the same GABA-based mechanism by which it mediates sensitivity to PTZ.

Considering that *rab-3(y251)* mutants (Figure 1, A and B; Figure 3, A–C; Nonet *et al.* 1997) and other PTZ-responsive general synaptic transmission mutants (Nguyen *et al.* 1995; Williams *et al.* 2004) are resistant to aldicarb, whereas systemic GABA mutants are PTZ responsive (Figure 1, A and B; Williams *et al.* 2004) and hypersensitive to aldicarb (Figure 3, A–C; Jiang *et al.* 2005; Vashlishan *et al.* 2008), these results are consistent with GABA-specific roles for our Rac-signaling pathway. As corroboration, heterotrimeric G-protein-signaling mutants, which are hypersensitive to aldicarb (Robatzek and Thomas 2000; Figure S2A) from excess secretion of ACh at NMJs, did not convulse on PTZ (Figure S2B). In fact, lf mutations in two antagonists of DGK-1 and GOA-1 activity, EGL-8 and EGL-10 (Robatzek and Thomas 2000), increased susceptibility to PTZ-induced anterior convulsions (Figure S1; Figure S2B; File S10), implying that GOA-1 inhibits RME activity.

To increase confidence in the interpretation of our pharmacological assays, we also placed young adult hermaphrodites in liquid and analyzed a high-frequency, drug-independent locomotory behavior known as "thrashing." Mutants lacking *egl-10* or other synaptic transmission genes have previously been shown to exhibit reduced thrashing rates (Miller *et al.* 1996). Despite hypersensitivity to aldicarb, *goa-1*(lf) mutants did not demonstrate thrashing rates significantly different from wild-type worms. Furthermore, *goa-1*(lf) mutants thrashed at significantly higher rates than the general synaptic transmission mutant [*rab-3(y251)*], a systemic GABA mutant [*unc-25(e156)*], Rac gf mutants, and Rac regulator mutants (Figure S2C). Surprisingly, thrashing assays have revealed another plausible explanation for the failure of *unc-25(e156)* mutants to spontaneously convulse. Although *unc-25(e156)* mutants had significantly lower thrashing rates (127.2 ± 17.5 thrashes/min) than wild-type worms (188.2 ± 14.8 thrashes/min), these systemic GABA mutants thrashed at significantly higher rates than *unc-49(e407)* mutants (96.5 ± 14.6 thrashes/min; Figure S2C), which have been shown to lack detectable inhibitory GABA transmission at body-wall muscles (Richmond and Jorgensen 1999). Perhaps *unc-25(e156)* mutants have

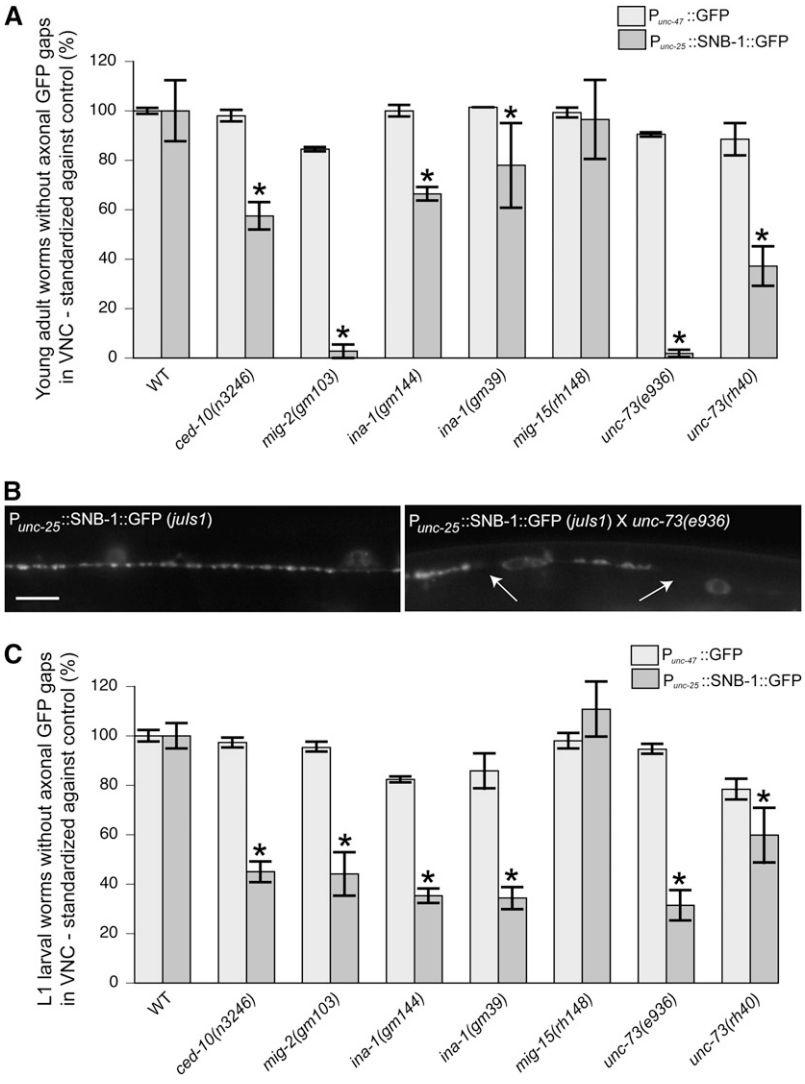

FIGURE 4.—Rac GTPase and canonical Rac regulator mutants exhibit synaptic vesicle misaccumulations, but not architectural breaks, in GABAergic D-type motor neurons of ventral nerve cords. (A) The percentage of axonal GFP gaps (the percentage of young adult worms with gaps per total sample size; $n = 30$ for each of three independent experiments) in GABAergic D-type motor neurons of ventral nerve cords (VNCs) in various *C. elegans* strains. Soluble GFP expression showed no architectural breaks in the VNC axons of wild-type (WT) or Rac-signaling-pathway mutant young adult *oxIs12* (P_{unc-47}::GFP) worms (dark gray bars). Yet, Rac-signaling mutants, except for hypomorphic *mig-15(rh148)* mutants, had misaccumulated synaptic vesicles, as revealed by gaps in GABAergic neuron-specific expression of a synaptobrevin-1 (SNB-1) and GFP translational fusion protein (light gray bars). Results from *oxIs12*-bearing Rac-signaling mutants were standardized against wild-type *oxIs*12 worms. Likewise, results from *juIs*1-bearing Rac-signaling mutants were standardized against wild-type *juIs1* (P_{unc-25}::SNB-1::GFP) worms. Each data point represents mean ± SD. $^*P < 0.05$; Fisher's exact test. The *ced-10(n3246)* mutants with *juIs1* are heterozygous for the dominant *n3246* allele, whereas *ced-10(n3246)* mutants with *oxIs12* are homozygous for the dominant *n3246* allele. (B) A representative wild-type *juIs1* young adult hermaphrodite exhibited no axonal SNB-1::GFP gaps, unlike an *unc-73(e936)* homozygote, which was deficient in Rac activation. (C) Soluble GFP expression revealed no significant architectural breaks in the VNC axons of wild-type, Rac gf, or Rac regulator mutant L1 larval *oxIs12* (P_{unc-47}::GFP) worms. GABAergic neuron-specific expression of a SNB-1 and GFP translational fusion protein in L1 larval GABAergic D-type motor neurons showed significant percentages of synaptic vesicle misaccumulations, as demonstrated by SNB-1::GFP gaps, in Rac gf, *ina-1(gm144), ina-1(gm39), unc-73(e936),* and *unc-73(rh40)* mutants. No axonal GFP gaps were observed in the VNCs of *mig-15(rh148)* mutant L1 larvae. Results from *oxIs12*-bearing Rac signaling mutants were standardized against wild-type *oxIs12* worms at the same developmental stage. Likewise, results from *juIs1*-bearing Rac signaling mutants were standardized against wild-type *juIs1* (P_{unc-25}::SNB-1::GFP) worms at the same developmental stage. Each data point represents mean ± SD. $^*P < 0.05$; Fisher's exact test. Asterisks for P_{unc-25}::SNB-1::GFP data indicate significant differences in percentages of axonal GFP gaps, compared to the wild-type *juIs1* background and P_{unc-47}::GFP data for the same mutant, suggesting that synaptic vesicle transport defects (SNB-1::GFP gaps) occur independently of architectural defects (soluble GFP gaps). Bar, 5 μm.

sufficient GABA production, which is undetectable by immunocytochemistry, in RMEs to prevent them from spontaneously convulsing. A different mutant with excess ACh secretion and associated hypersensitivity to aldicarb, *tom-1(ok188)* (McEwen *et al.* 2006), also failed to convulse in response to PTZ (Table 1) and thrashed at wild-type rates (185.3 ± 28.8 thrashes/min; $n = 30$ worms). These data imply that the dynein motor complex and Rac-signaling pathway control neuronal synchrony at *C. elegans* NMJs by promoting GABA transmission, not by negative regulation of ACh.

GABAergic synaptic vesicles misaccumulate in Rac-signaling mutants: Despite evidence that disruption of RMEs is most responsible for PTZ-induced convulsions, GABAergic synaptic vesicle misaccumulations in D-type motor neurons correlate well with PTZ sensitivity and are reliably scored (Williams *et al.* 2004; Locke *et al.* 2006). Our previous work demonstrates that misaccumulations of synaptic vesicles in GABAergic D-type motor neurons are associated with depletion of LIS-1 and dynein motor complex activity (Williams *et al.* 2004; Locke *et al.* 2006). Although Rac GTPase-signaling-pathway mutants mimic *lis-1* and dynein motor complex mutants in the presence of PTZ or aldicarb, we cannot assume that their sensitivities to these neural stimulants arise from a common mechanism. A Rac pathway functions in inhibitory GABAergic motor neuron development (Lundquist *et al.* 2001; Poinat *et al.* 2002; Lucanic *et al.* 2006). Thus, Rac pathway mutants may have increased susceptibilities to aldicarb

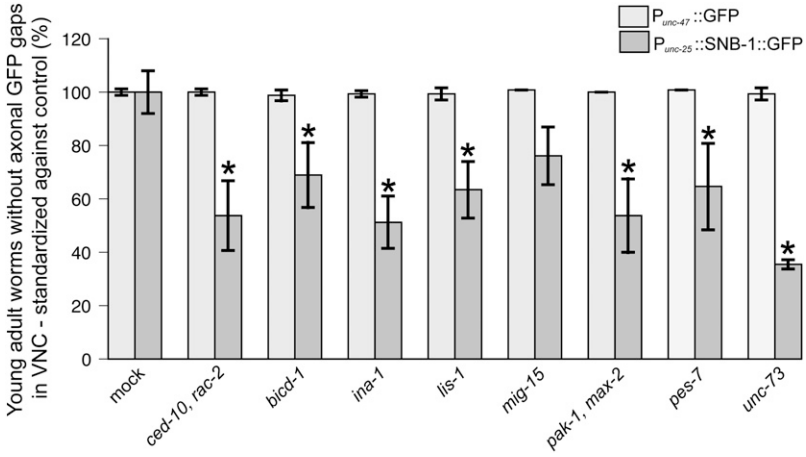

FIGURE 5.—Lactose-induced RNAi feeding against canonical Rac-signaling pathway members results in synaptic vesicle misaccumulations, but not architectural breaks, in GABAergic D-type motor neurons of ventral nerve cords. The percentage of axonal GFP gaps (the percentage of young adult worms with gaps per total sample size; $n = 30$ for each of three to five independent experiments) in GABAergic D-type motor neurons of ventral nerve cords (VNCs) of various RNAi treatments. Soluble GFP expression showed no architectural breaks in the VNC axons of young adult *oxIs12* (P_{unc-47}::GFP) worms with mock (α-synuclein) RNAi or RNAi against Rac-signaling-pathway members (dark gray bars). Yet, RNAi against Rac-signaling-pathway members, except for *mig-15*, resulted in misaccumulated synaptic vesicles, as revealed by gaps in GABAergic neuron-specific expression of a synaptobrevin-1 (SNB-1) and GFP translational fusion protein (light gray bars). Combinatorial RNAi was used against two of three triply redundant Racs, *ced-10* and *rac-2*. Results from mock RNAi against *oxIs12* worms were used to standardize other results with *oxIs*12 worms. Likewise, results from mock RNAi against *juIs*1 (P_{unc-25}::SNB-1::GFP) worms were used to standardize other results with *juIs1* worms. Each data point represents mean ± SD. $^*P < 0.05$; Fisher's exact test.

and/or PTZ as a result of architectural defects in the GABAergic nervous system.

To determine if a Rac pathway contributes to post-developmental GABAergic synaptic vesicle transport, we assayed for axonal gaps with SNB-1::GFP or soluble GFP expressed in GABAergic D-type motor neurons (Figure 4; Figure S3). To correlate axonal gaps with PTZ or aldicarb sensitivity, we first examined ventral nerve cords (VNCs; Figure 4A) and dorsal nerve cords (DNCs; Figure S3) of young adult hermaphrodites (WILLIAMS *et al.* 2004; LOCKE *et al.* 2006). However, axons from the two sets of GABAergic D-type motor neurons, known as VD and DD neurons, overlap extensively in the VNCs and DNCs of young adults. To buttress our analysis, we assayed VNCs of L1 larvae hermaphrodites for axonal GFP gaps whose VNCs contain only DD axons (SAKAMOTO *et al.* 2005; Figure 4C). Consistent with a role for triply redundant Racs and an integrin–NIK complex in mediating GABAergic D-type commissural navigation (POINAT *et al.* 2002), we observed significant soluble GFP gaps in DNCs of *mig-2(gm103)* young adult Rac gf mutants, in *ina-1(gm144)* and *mig-15(rh148)* young adult hypomorphs, and in Rac GEF-deficient (STEVEN *et al.* 1998), *unc-73(e936)* and *unc-73(rh40)* mutant young adults (Figure S3). Conversely, young adult mutants for either *ced-10(n3246)* or *ina-1(gm39)* did not exhibit significant soluble GFP gaps in their DNCs (Figure S3). Moreover, none of these Rac-signaling mutants had significant soluble GFP gaps in their VNCs, either as L1 larvae or as young adults (Figure 4).

All Rac-signaling mutants that we examined had significantly higher percentages of abnormally distributed synaptic vesicles, as revealed by SNB-1::GFP axonal gaps, than axon outgrowth defects, as revealed by soluble GFP (P_{unc-47}::GFP) gaps, in their VNCs at the young adult stage (Figure 4A) and at the L1 larval stage (Figure 4C). Figure 4B is a representative image showing SNB-1::GFP axonal gaps in the *unc-73(e936)* mutant background. We never observed SNB-1::GFP mislocalization in the DNCs of Rac-signaling mutant L1 larvae (data not shown), suggesting that this Rac-signaling pathway does not participate in synaptic vesicle cargo recognition during DD neuron remodeling (SAKAMOTO *et al.* 2005). The only Rac pathway mutants that did not exhibit significantly more SNB-1::GFP axonal gaps than soluble GFP gaps in young adult DNCs were the *mig-15* mutant, *rh148* (SHAKIR *et al.* 2006), and the strongest Rac GEF mutant, *rh40* (STEVEN *et al.* 1998) (Figure S3). Rac-signaling mutants had similar interpunctal SNB-1::GFP axonal gap widths and gap numbers at both L1 larval and young adult stages (Table S1). Thus, SNB-1::GFP axonal gap frequencies, not interpunctal widths or numbers, correlate with Rac-signaling mutant sensitivities to PTZ and aldicarb.

Because significantly reduced SNB-1::GFP gaps in the majority of the Rac pathway mutants tested could not be explained by axon outgrowth defects, these data suggest that synaptic vesicle misaccumulations in GABAergic motor neurons could be sufficient for enhanced sensitivities of Rac pathway mutants to aldicarb and PTZ. In support of this hypothesis, *ina-1(gm39)* mutants, unlike *ina-1(gm144)* mutants, had insignificant architectural defects in GABAergic DD motor neurons of young adults (Figure S3). Yet, *ina-1(gm39)* mutants were more sensitive to aldicarb (Figure 3C) and PTZ (Figure 1B) than *ina-1(gm144)* mutants. Defects in non-GABAergic neurons of the stronger mutant might explain its weaker sensitivities to aldicarb and PTZ. However, paralysis from severe defects in synaptic transmission or axon pathfinding does not prevent PTZ-induced convulsions, since 100.0% of *unc-26(e1196)* and 82.2% of *unc-51(e396)* immotile mutants exhibited

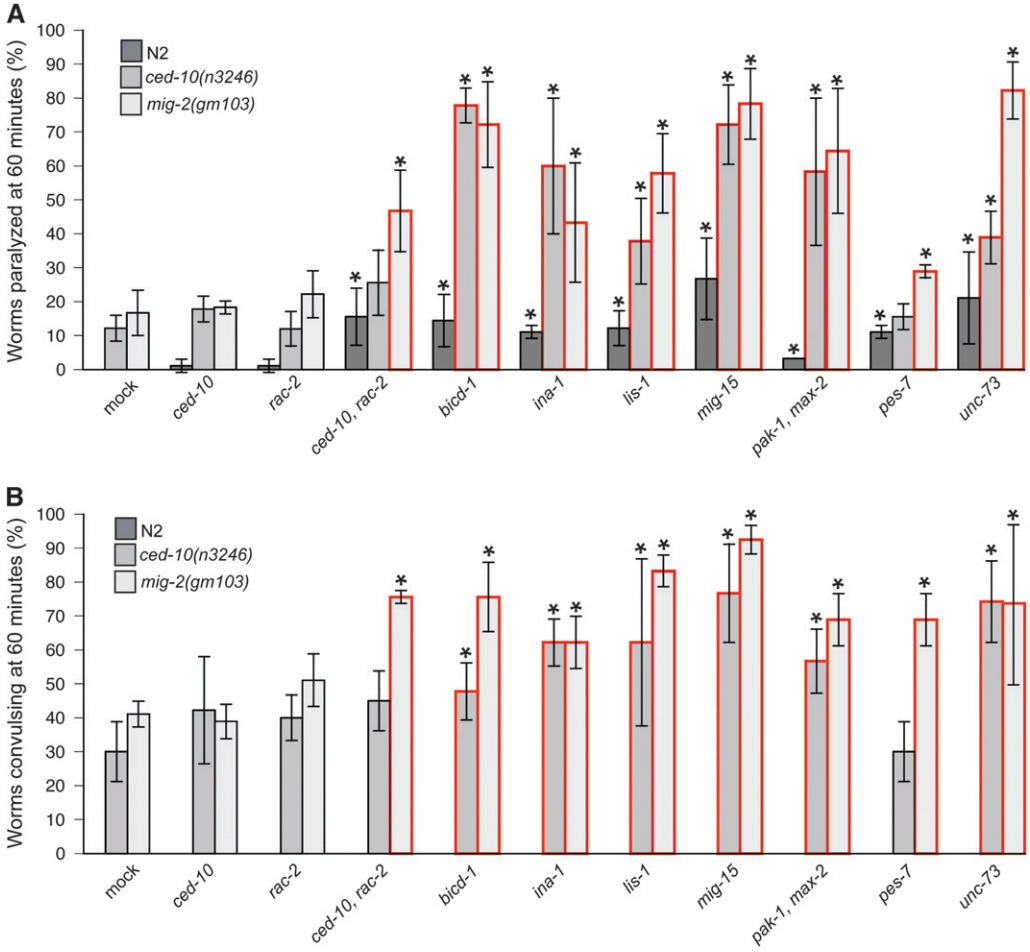

FIGURE 6.—RNAi feeding and pharmacological assays with Rac GTPase mutant backgrounds reveal synergistic genetic interactions with the dynein motor complex and canonical Rac regulators. (A and B) The response level (the percentage of young adult worms paralyzed per total sample size; $n = 30$ for each of three to five independent experiments) of various RNAi treatments after 60 min of exposure to aldicarb (A) or PTZ (B). (A) Like mock (α-synuclein) RNAi, RNAi against triply redundant Rac, *ced-10*, or *rac-2* was not sufficient to enhance aldicarb sensitivity of N2 wild-type worms (dark gray bars). Conversely, combinatorial RNAi against *ced-10* (medium gray bars) and *rac-2* (light gray bars) was sufficient to enhance aldicarb sensitivity of wild-type worms. Similar enhancements of N2 sensitivity to aldicarb were observed with RNAi against the canonical Rac regulators, *ina-1*, *mig-15*, *pes-7*, or *unc-73*. Combinatorial RNAi against the functionally redundant PAK orthologs, *pak-1* and *max-2*, or RNAi against the dynein motor complex members, *bicd-1* and *lis-1*, was also sufficient to increase N2 sensitivity to aldicarb. RNAi against most of these Rac-signaling-pathway or dynein motor complex members also enhanced aldicarb sensitivities of either or both Rac gain-of-function mutants, *ced-10(n3246)* and *mig-2(gm103)*. RNAi against either *ced-10* or *rac-2* was not sufficient to enhance the aldicarb sensitivity of either Rac gain-of-function mutant, while *pes-7*(RNAi) enhanced aldicarb sensitivity of *mig-2(gm103)*, but not of *ced-10(n3246)*. (B) The same synergistic genetic interactions, which were uncovered with aldicarb exposure, were confirmed with PTZ exposure. Yet, RNAi against wild-type worms was not sufficient to yield convulsions. Each data point represents mean ± SD. $*P < 0.05$; Fisher's exact test. Asterisks indicate enhancement, compared to mock RNAi against a given genotypic background. Red outlines around bars indicate synergism, in which RNAi against a mutant background results in greater drug sensitivity than the sum of the same RNAi treatment against a wild-type background and mock RNAi against the same mutant.

anterior convulsions with 2.5 mg/ml PTZ. As noted above, *gm39* may also affect binding of a different number and/or class of ligands than *gm144*. Regardless, similar synaptic vesicle misaccumulations suggest that LIS-1 and dynein converge with Racs to control GABA transmission at adult *C. elegans* NMJs.

RNAi confirms role for Rac-signaling pathway in GABAergic vesicle transport: SNB-1::GFP misaccumulations implicate Rac signaling in GABAergic vesicle transport. Yet, these data are difficult to interpret in light of subtle axon-pathfinding defects in GABAergic D-type motor neurons. To be confident that GABAergic vesicle transport defects from Rac signaling attenuation are not secondary to axon-pathfinding defects, we used RNAi to produce weaker phenotypes than those of extant mutants.

We have previously shown that lactose-induced RNAi feeding against LIS-1 pathway members is sufficient to cause SNB-1::GFP misaccumulations in D-type motor neurons (LOCKE *et al.* 2006). Accordingly, lactose-induced RNAi feeding uncovered GABAergic vesicle transport abnormalities, which phenocopied *lis-1(t1550)* and Rac-signaling-pathway mutants, with combinatorial RNAi (TISCHLER *et al.* 2006) against both *ced-10* and *rac-2* (Figure 5; Figure S4) in first generation (F_1) progeny of RNAi-treated worms. As with the mutant alleles, SNB-1::GFP misaccumulated with *mig-15*(RNAi) in DNCs and with *ina-1*(RNAi), *lis-1*(RNAi), or *unc-73*(RNAi) in both VNCs and DNCs (Figure 5; Figure S4) of F_1 progeny. RNAi feeding also revealed SNB-1::GFP misaccumulations with combinatorial RNAi against the functionally redundant *C. elegans* PAK orthologs, *pak-1* and *max-2* (Figure 5; Figure S4), that encode the immediate downstream effectors of activated Racs implicated in GABAergic D-type commissural axon

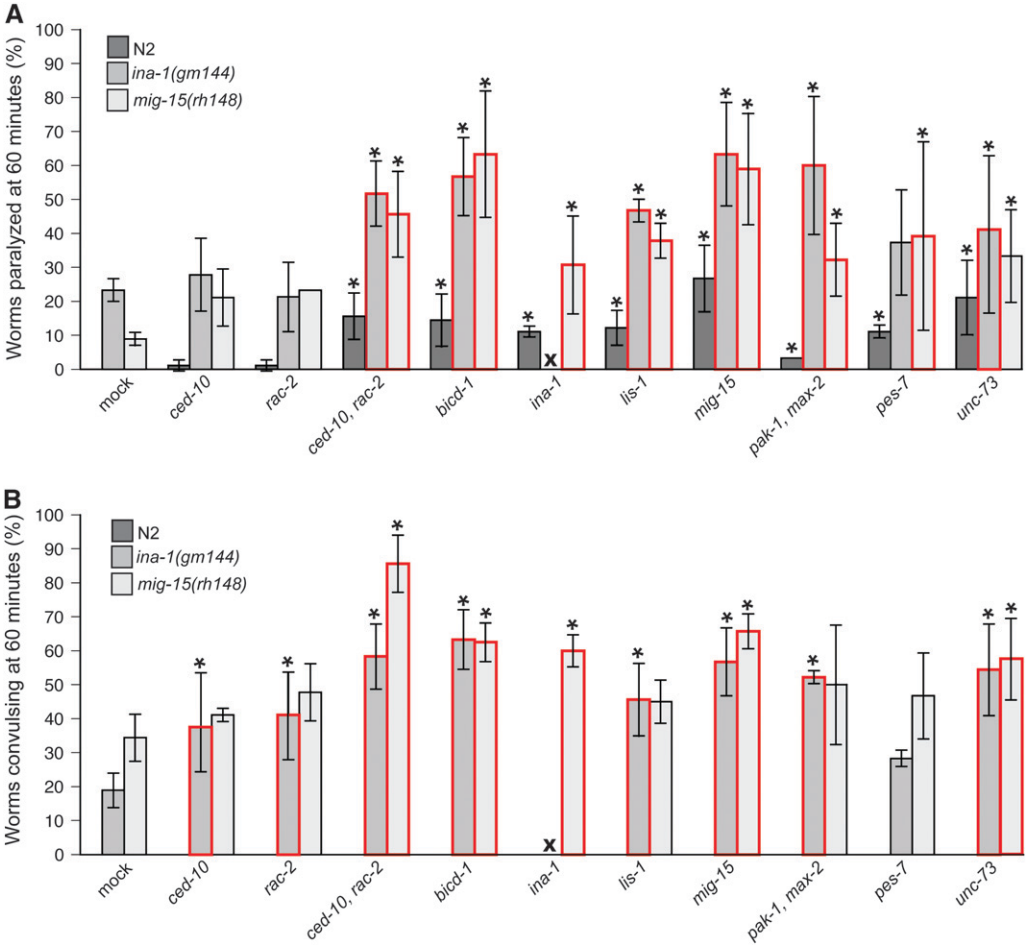

FIGURE 7.—RNAi feeding and pharmacological assays with hypomorphic Rac regulator mutant backgrounds reveal synergistic genetic interactions with the dynein motor complex and canonical Rac regulators. (A and B) The response level (the percentage of young adult worms paralyzed per total sample size; $n = 30$ for each of three to five independent experiments) of various RNAi treatments after 60 min of exposure to aldicarb (A) or PTZ (B). All RNAi treatments against N2 wild-type worms are repeated from Figure 6 for convenience (dark gray bars). As denoted by "X", lethality resulted from *ina-1*(RNAi) against *ina-1(gm144)* mutants, precluding analysis. (A) RNAi against most of the Rac-signaling-pathway or dynein motor complex members enhanced aldicarb sensitivities of either or both Rac regulator mutants, *ina-1(gm144)* (medium gray bars) and *mig-15(rh148)* (light gray bars). Unlike combinatorial RNAi against both genes, RNAi against the redundant Racs *ced-10* or *rac-2* was not sufficient to enhance the aldicarb sensitivity of either Rac regulator mutant. RNAi against *pes-7* enhanced aldicarb sensitivity of *mig-15(rh148)*, but not of *ina-1(gm144)*, whereas *unc-73*(RNAi) enhanced aldicarb sensitivity of *ina-1(gm144)*, but not of *mig-15(rh148)*. (B) The same synergistic genetic interactions that were uncovered with aldicarb were confirmed with PTZ. Unlike the results from aldicarb exposure, RNAi against either *ced-10* or *rac-2* was sufficient to enhance PTZ-induced anterior convulsions of *ina-1(gm144)* mutants, but not of *mig-15(rh148)*. PTZ exposure also did not reveal synergistic genetic interactions between *mig-15* and *lis-1*, *pes-7*, or the PAK orthologs *pak-1* and *max-2*. Yet, *unc-73*(RNAi) enhanced *mig-15(rh148)* convulsions, revealing interactions that were not apparent from aldicarb exposure. Each data point represents mean ± SD. $^*P < 0.05$; Fisher's exact test. Asterisks indicate enhancement, compared to mock RNAi against a given genotypic background. Red outlines around bars indicate synergism, in which RNAi against a mutant background results in greater drug sensitivity than the sum of the same RNAi treatment against a wild-type background and mock RNAi against the same mutant.

navigation (LUCANIC *et al.* 2006). These results may suggest that PAK-mediated signals between actin and microtubule networks are particularly important for GABAergic vesicle transport, as dynein motor complex subunits, such as dynein light chain (LU *et al.* 2005) and dynamitin (MENZEL *et al.* 2007), have also been shown to physically interact with PAK orthologs in humans and Drosophila, respectively.

Additionally, our results suggest novel roles for *bicd-1*, the worm ortholog of bicaudal-D, a dynein- and NIK-interacting protein (HOUALLA *et al.* 2005), and *pes-7*, the worm ortholog of IQGAP1, a rodent Lis1 and Rac1 interactor (KHOLMANSKIKH *et al.* 2006), in GABAergic vesicle transport (Figure 5; Figure S4). RNAi against these genes did not result in soluble GFP axonal gaps (Figure 5; Figure S4). In contrast, most of the same RNAi treatments against parent animals, instead of their F_1 progeny, resulted in SNB-1::GFP misaccumulations, but not soluble GFP axonal gaps (Figure S5), such as those observed with young adult Rac-signaling mutants (Table S1). The only treatment that did not uncover a trend toward GABAergic vesicle transport defects was combinatorial RNAi against *pak-1* and *max-2* in parents (Figure S5). This result may be explained by dilution of phenotypic strength, where RNAi phenotypes are weakened by multiple gene targeting (TISCHLER *et al.* 2006).

RNAi reveals synergistic interactions between dynein and Rac-signaling pathways: To determine if members of a canonical Rac-signaling pathway function together to modulate neuronal synchrony in *C. elegans*, we performed aldicarb-induced paralysis assays and PTZ-

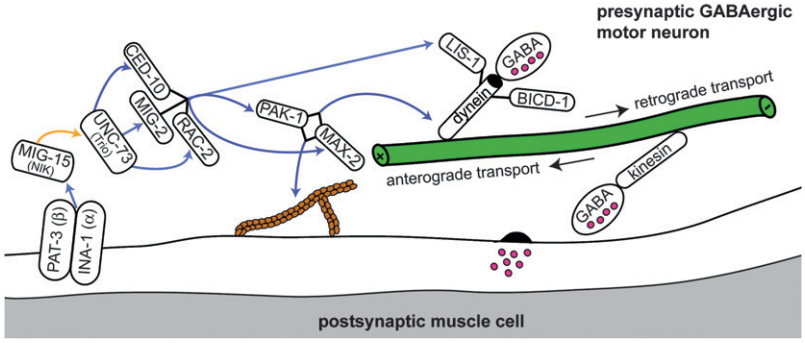

FIGURE 8.—Model depicting a potential role for a Rac GTPase-signaling pathway in dynein-mediated synaptic vesicle transport in *en passant C. elegans* GABAergic motor axons. Triply redundant Racs (CED-10, MIG-2, and RAC-2) and their activator, UNC-73 (Trio), may transmit extracellular signals from a Nck-interacting kinase (MIG-15), α-integrin (INA-1), and β-integrin (PAT-3) complex to a PAK-mediated interface between actin and microtubule networks. Redundant worm PAK orthologs (PAK-1 and MAX-2) may promote dynein motility through physical interactions with dynein motor complex subunits and/or actin. BICD-1 may regulate vesicle transport via physical interactions with dynein. LIS-1 may also regulate dynein motor activity through direct physical interactions with dynein motor complex subunits and/or Racs. These interactions may be involved in coordinating the binding of GABAergic synaptic vesicles at microtubule plus ends and subsequent retrograde transport. Disrupting these interactions could also lead to anterograde transport defects, due to the putative interdependency of dynein and kinesin, and to diminished levels of inhibitory GABA secretion. Blue arrows indicate that physical and genetic interactions have been shown. Orange arrows indicate that only a genetic interaction has been observed. Microtubules are shown in green, while F-actin is shown in brown. GABA is colored purple.

induced convulsion assays with RNAi-treated animals. Consistent with parallel functions of triply redundant Racs in GABAergic motor neurons (LUNDQUIST *et al.* 2001), RNAi against *ced-10* in *mig-2(gm103)* gf mutants was not sufficient to alter sensitivity to aldicarb (Figure 6A). Likewise, RNAi against *rac-2* in either *ced-10(n3246)* or *mig-2(gm103)* gf mutant backgrounds was not sufficient to alter aldicarb sensitivity (Figure 6A). However, combinatorial RNAi against *ced-10* and *rac-2* synergized with a *mig-2(gm103)* mutation to significantly enhance aldicarb sensitivity and was also sufficient to increase aldicarb sensitivity of N2 wild-type worms (Figure 6A).

RNAi against *bicd-1*, *ina-1*, *lis-1*, *mig-15*, *pes-7*, or *unc-73*, as well as combinatorial RNAi against the functionally redundant *pak-1* and *max-2* genes, was sufficient to enhance the aldicarb sensitivity of wild-type worms (Figure 6A). RNAi against these putative Rac-signaling-pathway members, except for *pes-7* with *ced-10(n3246)*, resulted in synergistic enhancement of sensitivity to aldicarb in both Rac gf mutant backgrounds (Figure 6A). Despite not being sufficient to induce anterior convulsions in the presence of PTZ, as predicted by our earlier studies (LOCKE *et al.* 2006), these same RNAi treatments also synergized with Rac gf mutations to increase sensitivity to PTZ-induced anterior convulsions (Figure 6B). Furthermore, most of these RNAi treatments synergized with hypomorphic *ina-1(gm144)* and *mig-15(rh148)* mutations, albeit weakly with the latter, to increase sensitivity to aldicarb (Figure 7A) and PTZ (Figure 7B). Specifically, neither RNAi against *lis-1*, *pes-7*, and *unc-73* nor combinatorial RNAi against *pak-1* and *max-2* was sufficient to significantly enhance sensitivity to PTZ with *mig-15(rh148)* (Figure 7B). Likewise, *pes-7*(RNAi) was not sufficient to significantly enhance sensitivity to aldicarb (Figure 7A) or PTZ with *ina-1(gm144)* (Figure 7B). These inconsistencies could result from our use of weaker hypomorphic mutants (POINAT *et al.* 2002) or subthreshold levels of neural stimulants. Ultimately, however, these results suggest that the canonical Rac GTPase regulators, INA-1, MIG-15, UNC-73, PAK-1, and MAX-2, modulate neuronal synchrony through interactions with triply redundant Racs, integrators of microtubule-actin-signaling networks, such as LIS-1, PES-7, and BICD-1.

DISCUSSION

We previously reported that disturbance of LIS-1 and the dynein motor complex results in enhanced sensitivities to a $GABA_A$ receptor antagonist, PTZ, and synaptic vesicle misaccumulations, which were specific to GABAergic motor neurons (WILLIAMS *et al.* 2004; LOCKE *et al.* 2006). In this work, we show that both *lis-1* and *dhc-1* mutants are also hypersensitive to an acetylcholinesterase inhibitor, aldicarb, which overstimulates body-wall muscles (NGUYEN *et al.* 1995; MILLER *et al.* 1996) in a similar manner to PTZ. These results further suggest that *lis-1* and *dhc-1* cooperate with GABA to modulate neuronal synchrony. Yet, these data do not suggest a mechanism by which LIS-1 and dynein may function specifically in *C. elegans* GABA transmission, given their pleiotropy and likely roles in general synaptic function. Here, we present evidence that this mechanism is Rac dependent and active in diverse sets of GABAergic neurons.

GABAergic D-type motor neurons are known to complete their development in the second of four *C. elegans* larval stages (KNOBEL *et al.* 1999). Moreover, previous studies have demonstrated that a tripartite Rac GTPase-signaling cascade mediates commissural axon navigation of these neurons (LUNDQUIST *et al.* 2001; POINAT *et al.* 2002; LUCANIC *et al.* 2006). Interestingly, expression of *C. elegans* Racs persists in the adult GABAergic nervous system (LUNDQUIST *et al.* 2001). Rac regulators, including *ina-1* (BAUM and GARRIGA 1997), *mig-15* (POINAT *et al.* 2002), and *unc-73* (STEVEN *et al.* 1998; HUNT-NEWBURY *et al.* 2007), as well as *lis-1*

(Dawe *et al.* 2001; Hunt-Newbury *et al.* 2007) and *dhc-1* (Hunt-Newbury *et al.* 2007), have also been detected in GABAergic neurons of adult *C. elegans* hermaphrodites. These findings suggest that a Rac-signaling pathway could govern not only GABAergic neuron development but also GABA transmission, post-developmentally. Consistent with this hypothesis, we show for the first time that a Rac-signaling pathway modulates synaptic transmission at adult *C. elegans* NMJs. Furthermore, we present evidence that Racs have post-developmental functions, which appear distinct from previously described neuromuscular roles for RHO-1 (McMullan *et al.* 2006; Williams *et al.* 2007). More specifically, this Rac cascade is required for dynein-mediated synaptic vesicle transport in GABAergic neurons.

Rho family GTPases, including Racs, may be differentially regulated in space and time to confer cellular identity (de Curtis 2008). Indeed, disparate Rac-signaling pathways have been implicated in several *C. elegans* developmental processes (Lundquist *et al.* 2001). Here, we reveal a specific role for an integrin-mediated tripartite Rac cascade in GABAergic motor neurons by combining microscopic, pharmacological, and behavioral approaches. Furthermore, we have shown that Rac regulators, which were previously implicated in GABAergic D-type motor neuron commissural axon navigation (Poinat *et al.* 2002), genetically interact with Racs and the dynein motor complex to mediate GABAergic vesicle transport. We have also identified roles for *C. elegans* orthologs of bicaudal-D and IQGAP1 in this dynein–Rac-signaling pathway. It has been speculated that these genes integrate signals between microtubule and actin networks via NIK and Lis1, respectively (Houalla *et al.* 2005; Kholmanskikh *et al.* 2006). Although our results support these propositions, a series of *bicd-1* and *pes-7* hypomorphic and null mutant alleles will be required to fully understand the neuronal functions of these genes.

On the basis of the above results, we present a model in which disruption of this dynein–Rac-signaling pathway results in a loss of the axonal transport of synaptic vesicles in GABAergic motor neurons (Figure 8). As suggested in Figure 8, it is plausible that this dynein–Rac-signaling pathway coordinates microtubule plus end-binding of GABAergic synaptic vesicles, thereby allowing them to undergo retrograde transport. Evidence for the interdependency of dynein and kinesin in anterograde transport also exists and likely explains the GABAergic vesicle misaccumulations and associated behavioral phenotypes, which we observed (Williams *et al.* 2004; Locke *et al.* 2006). These GABAergic vesicle misaccumulations could also be caused by disruptions in other cellular processes, such as the localization of SNB-1::GFP to synaptic vesicle membranes, selective degeneration or retraction of axons, or regulated degradation or endocytosis of SNB-1::GFP (Koushika *et al.* 2004). We hypothesize that SNB-1::GFP misaccumulates in these dynein–Rac-signaling mutants due to axonal transport defects. However, these alternative hypotheses could be considered in the future, perhaps best with live imaging.

The identification and characterization of interactions between Racs and the dynein motor complex was accomplished by separating the architectural from the functional defects in GABAergic neurons and knocking down putative interactors in sensitized genotypic backgrounds. To this end, we employed lactose-induced RNAi feeding, which dependably inhibits gene expression in GABAergic motor neurons (Locke *et al.* 2006). We found that RNAi against members of a Rac cascade was not sufficient to cause architectural defects in the GABAergic nervous system, even though these genes are important for GABAergic D-type motor neuron development (Lundquist *et al.* 2001; Poinat *et al.* 2002; Lucanic *et al.* 2006). Conversely, RNAi against these targets was sufficient to cause SNB-1::GFP misaccumulations, revealing a link with synaptic vesicle transport. RNAi feeding in hypomorphic genotypic backgrounds was sufficient to uncover genetic interactions without the need to cross mutants with slow-growing hypersensitive RNAi strains. This approach may be used to accelerate the mapping of other signaling cascades and to identify roles for other developmental genes in adult neurons.

Previous studies with *C. elegans* and other model systems have postulated interactions between the dynein motor complex and Rac GTPases. For example, an integrin-dependent signaling cascade has been shown to mediate trafficking of lipid rafts through Rac1, Arf6, and microtubules (Balasubramanian *et al.* 2007). Likewise, inhibition of Dictyostelium orthologs of LIS-1 and dynein intermediate chain has been associated with actin depolymerization, possibly through disruption of Rac1 (Rehberg *et al.* 2005). Consistent with these results, a *C. elegans* study has shown that *lis-1* and *dhc-1* mutants are defective in germline cell corpse engulfment (Buttner *et al.* 2007). Although the molecular basis of these engulfment defects was not investigated, the data suggested that corpse engulfment is dynein dependent and likely required *lis-1* and *dhc-1* for cargo transport and/or changes in cytoskeletal dynamics (Buttner *et al.* 2007). These hypotheses are particularly relevant to our own findings, as one of three *C. elegans* Racs, CED-10, is essential for corpse engulfment (Kinchen *et al.* 2005). It is possible that dynein and LIS-1 cooperate with CED-10 and other Rac regulators to mediate engulfment. However, it is unlikely that the CED-10-dependent mechanism, which is necessary for engulfment, is the same one responsible for neuronal synchronization and dynein-mediated GABAergic vesicle transport. Indeed, null mutants of *ced-2* and *ced-5*, both of which are important regulators of CED-10 in engulfment (Ellis *et al.* 1991), exhibited wild-type sensitivities to the $GABA_A$ receptor antagonist PTZ

(Table 1). Thus, a unique and perhaps uncharacterized set of Rac regulators could govern Rac and dynein activity in adult GABAergic neurons.

Perturbations of inhibitory GABA transmission can promote epileptic activity in a wide range of model systems, including rodents (Delorey *et al.* 1998), zebrafish (Baraban *et al.* 2005), Drosophila (Pavlidis *et al.* 1994; Guan *et al.* 2005), and *C. elegans* (Williams *et al.* 2004). These studies underscore the utility of both mammalian and non-mammalian models to reveal cellular effectors of neuronal activity (Locke *et al.* 2009). Accordingly, several reports from a variety of animal models further implicate members of a Rac-signaling pathway in seizures and epilepsy. Orthologs of *dhc-1*, *lis-1*, the functionally redundant Racs and Paks, *ina-1*, *mig-15*, *unc-73*, *bicd-1*, and *pes-7* are all expressed in GABA-enriched regions of the adult mouse brain (Lein *et al.* 2007). In addition, limbic seizures have been shown to result in increased expression levels of integrin β 1 (Pinkstaff *et al.* 1998) and NIK (Arion *et al.* 2006), while integrins have been shown to modulate long-term potentiation in a mature hippocampus (Chan *et al.* 2006; Huang *et al.* 2006). Seizure-like activity in Drosophila has also been shown to induce α-integrin and trio expression and to downregulate a Rac-GAP (Guan *et al.* 2005). Together with our own findings, these data strongly suggest the plausibility of an evolutionarily conserved network of cytoskeletal regulators that cooperate in the maintenance of a GABA-dependent seizure threshold.

We thank all members of the Caldwell Laboratory, especially Laura Berkowitz, Lindsay Faircloth, Stacey Fox, and David Agee for their collegiality and teamwork. Particular thanks also go to Hwai-Jong Cheng, Gian Garriga, Yishi Jin, Erik Jorgensen, and Erik Lundquist for donating *C. elegans* strains. All *C. elegans* mutants came from the Caenorhabditis Genetics Center, which is funded by the National Institutes of Health National Center for Research Resources. An Undergraduate Science Education Program grant from the Howard Hughes Medical Institute supported the undergraduate researchers (K.P.B. and S.K.L.) involved in this study. Additional support came from a National Science Foundation CAREER Award to G.A.C.

LITERATURE CITED

Arion, D., M. Sabatini, T. Unger, J. Pastor, L. Alonso-Nanclares *et al.*, 2006 Correlation of transcriptome profile with electrical activity in temporal lobe epilepsy. Neurobiol. Dis. **22:** 374–387.

Balasubramanian, N., D. W. Scott, J. D. Castle, J. E. Casanova and M. A. Schwartz, 2007 Arf6 and microtubules in adhesion-dependent trafficking of lipid rafts. Nat. Cell Biol. **9:** 1381–1391.

Baraban, S. C., M. R. Taylor, P. A. Castro and H. Baier, 2005 Pentylenetetrazole induced changes in zebrafish behavior, neural activity and c-fos expression. Neuroscience **131:** 759–768.

Baum, P. D., and G. Garriga, 1997 Neuronal migrations and axon fasciculation are disrupted in *ina-1* integrin mutants. Neuron **19:** 51–62.

Brenner, S., 1974 The genetics of *Caenorhabditis elegans*. Genetics **77:** 95–104.

Brill, J., M. Lee, S. Zhao, R. D. Fernald and J. R. Huguenard, 2006 Chronic valproic acid treatment triggers increased neuropeptide y expression and signaling in rat nucleus reticularis thalami. J. Neurosci. **26:** 6813–6822.

Buttner, E. A., A. J. Gil-Krzewska, A. K. Rajpurohit and C. P. Hunter, 2007 Progression from mitotic catastrophe to germ cell death in *Caenorhabditis elegans lis-1* mutants requires the spindle checkpoint. Dev. Biol. **305:** 397–410.

Cardoso, C., R. J. Leventer, J. J. Dowling, H. L. Ward, J. Chung *et al.*, 2002 Clinical and molecular basis of classical lissencephaly: mutations in the *LIS1* gene (*PAFAH1B1*). Hum. Mutat. **19:** 4–15.

Chan, C. S., E. J. Weeber, L. Zong, E. Fuchs, J. D. Sweatt *et al.*, 2006 Beta 1-integrins are required for hippocampal AMPA receptor-dependent synaptic transmission, synaptic plasticity, and working memory. J. Neurosci. **26:** 223–232.

Cobos, I., M. E. Calcagnotto, A. J. Vilaythong, M. T. Thwin, J. L. Noebels *et al.*, 2005 Mice lacking Dlx1 show subtype-specific loss of interneurons, reduced inhibition and epilepsy. Nat. Neurosci. **8:** 1059–1068.

Cossette, P., L. Liu, K. Brisebois, H. Dong, A. Lortie *et al.*, 2002 Mutation of *GABRA1* in an autosomal dominant form of juvenile myoclonic epilepsy. Nat. Genet. **31:** 184–189.

Dalpé, G., L. W. Zhang, H. Zheng and J. G. Culotti, 2004 Conversion of cell movement responses to semaphorin-1 and plexin-1 from attraction to repulsion by lowered levels of specific RAC GTPases in *C. elegans*. Development **131:** 2073–2088.

Dawe, A. L., P. M. Harris, N. R. Morris and G. A. Caldwell, 2001 Evolutionarily conserved nuclear migration genes required for early embryonic development in *Caenorhabditis elegans*. Dev. Genes Evol. **211:** 434–441.

de Curtis, I., 2008 Functions of Rac GTPases during neuronal development. Dev. Neurosci. **30:** 47–58.

DeLorey, T. M., A. Handforth, S. G. Anagnostaras, G. E. Homanics, B. A. Minassian *et al.*, 1998 Mice lacking the beta3 subunit of the GABAA receptor have the epilepsy phenotype and many of the behavioral characteristics of Angelman syndrome. J. Neurosci. **18:** 8505–8514.

Dent, J. A., M. M. Smith, D. K. Vassilatis and L. Avery, 2000 The genetics of ivermectin resistance in *Caenorhabditis elegans*. Proc. Natl. Acad. Sci. USA **97:** 2674–2679.

Di Cunto, F., S. Imarisio, E. Hirsch, V. Broccoli, A. Bulfone *et al.*, 2000 Defective neurogenesis in citron kinase knockout mice by altered cytokinesis and massive apoptosis. Neuron **28:** 115–127.

Di Paolo, G., S. Sankaranarayanan, M. R. Wenk, L. Daniell, E. Perucco *et al.*, 2002 Decreased synaptic vesicle recycling efficiency and cognitive deficits in amphiphysin 1 knockout mice. Neuron **33:** 789–804.

Ellis, R. E., D. M. Jacobson and H. R. Horvitz, 1991 Genes required for the engulfment of cell corpses during programmed cell death in *Caenorhabditis elegans*. Genetics **129:** 79–94.

Etter, A., D. F. Cully, K. K. Liu, B. Reiss, D. K. Vassilatis *et al.*, 1999 Picrotoxin blockade of invertebrate glutamate-gated chloride channels: subunit dependence and evidence for binding within the pore. J. Neurochem. **72:** 318–326.

Fernandez, F., W. Morishita, E. Zuniga, J. Nguyen, M. Blank *et al.*, 2007 Pharmacotherapy for cognitive impairment in a mouse model of Down syndrome. Nat. Neurosci. **10:** 411–413.

Gitai, Z., T. W. Yu, E. A. Lundquist, M. Tessier-Lavigne and C. I. Bargmann, 2003 The netrin receptor UNC-40/DCC stimulates axon attraction and outgrowth through enabled and, in parallel, Rac and UNC-115/AbLim. Neuron **37:** 53–65.

Guan, Z., S. Saraswati, B. Adolfsen and J. T. Littleton, 2005 Genome-wide transcriptional changes associated with enhanced activity in the *Drosophila* nervous system. Neuron **48:** 91–107.

Houalla, T., D. Hien Vuong, W. Ruan, B. Suter and Y. Rao, 2005 The Ste20-like kinase misshapen functions together with Bicaudal-D and dynein in driving nuclear migration in the developing Drosophila eye. Mech. Dev. **122:** 97–108.

Huang, R. Q., C. L. Bell-Horner, M. I. Dibas, D. F. Covey, J. A. Drewe *et al.*, 2001 Pentylenetetrazole-induced inhibition of recombinant gamma-aminobutyric acid type A (GABA(A)) receptors: mechanism and site of action. J. Pharmacol. Exp. Ther. **298:** 986–995.

Huang, Z., K. Shimazu, N. H. Woo, K. Zang, U. Muller *et al.*, 2006 Distinct roles of the beta 1-class integrins at the developing and the mature hippocampal excitatory synapse. J. Neurosci. **26:** 11208–11219.

Hunt-Newbury, R., R. Viveiros, R. Johnsen, A. Mah, D. Anastas *et al.*, 2007 High-throughput in vivo analysis of gene expression in *Caenorhabditis elegans*. PLoS Biol. **5:** e237.

Jiang, G., L. Zhuang, S. Miyauchi, K. Miyake, Y. J. Fei *et al.*, 2005 A Na+/Cl− -coupled GABA transporter, GAT-1, from *Caenorhabditis elegans*: structural and functional features, specific expression in GABA-ergic neurons, and involvement in muscle function. J. Biol. Chem. **280:** 2065–2077.

Jin, Y., R. Hoskins and H. R. Horvitz, 1994 Control of type-D GABAergic neuron differentiation by *C. elegans* UNC-30 homeodomain protein. Nature **372:** 780–783.

Kamath, R. S., A. G. Fraser, Y. Dong, G. Poulin, R. Durbin *et al.*, 2003 Systematic functional analysis of the *Caenorhabditis elegans* genome using RNAi. Nature **421:** 231–237.

Keane, J., and L. Avery, 2003 Mechanosensory inputs influence *Caenorhabditis elegans* pharyngeal activity via ivermectin sensitivity genes. Genetics **164:** 153–162.

Keays, D. A., G. Tian, K. Poirier, G. J. Huang, C. Siebold *et al.*, 2007 Mutations in alpha-tubulin cause abnormal neuronal migration in mice and lissencephaly in humans. Cell **128:** 45–57.

Kholmanskikh, S. S., J. S. Dobrin, A. Wynshaw-Boris, P. C. Letourneau and M. E. Ross, 2003 Disregulated RhoGTPases and actin cytoskeleton contribute to the migration defect in Lis1-deficient neurons. J. Neurosci. **23:** 8673–8681.

Kholmanskikh, S. S., H. B. Koeller, A. Wynshaw-Boris, T. Gomez, P. C. Letourneau *et al.*, 2006 Calcium-dependent interaction of Lis1 with IQGAP1 and Cdc42 promotes neuronal motility. Nat. Neurosci. **9:** 50–57.

Kinchen, J. M., J. Cabello, D. Klingele, K. Wong, R. Feichtinger *et al.*, 2005 Two pathways converge at CED-10 to mediate actin rearrangement and corpse removal in *C. elegans*. Nature **434:** 93–99.

Kishore, R. S., and M. V. Sundaram, 2002 *ced-10* Rac and *mig-2* function redundantly and act with *unc-73* trio to control the orientation of vulval cell divisions and migrations in *Caenorhabditis elegans*. Dev. Biol. **241:** 339–348.

Knobel, K. M., E. M. Jorgensen and M. J. Bastiani, 1999 Growth cones stall and collapse during axon outgrowth in *Caenorhabditis elegans*. Development **126:** 4489–4498.

Koushika, S. P., A. M. Schaefer, R. Vincent, J. H. Willis, B. Bowerman *et al.*, 2004 Mutations in *Caenorhabditis elegans* cytoplasmic dynein components reveal specificity of neuronal retrograde cargo. J. Neurosci. **24:** 3907–3916.

Lein, E. S., M. J. Hawrylycz, N. Ao, M. Ayres, A. Bensinger *et al.*, 2007 Genome-wide atlas of gene expression in the adult mouse brain. Nature **445:** 168–176.

Locke, C. J., S. N. Williams, E. M. Schwarz, G. A. Caldwell and K. A. Caldwell, 2006 Genetic interactions among cortical malformation genes that influence susceptibility to convulsions in *C. elegans*. Brain Res. **1120:** 23–34.

Locke, C. J., K. Berry, B. Kautu, K. Lee and K. Caldwell *et al.*, 2008 Paradigms for pharmacological characterization of *C. elegans* synaptic transmission mutants. J. Vis. Exp., **18:** 837.

Locke, C. J., K. A. Caldwell and G. A. Caldwell, 2009 The nematode, *C. elegans*, as an emerging model of seizures and epilepsy, pp. 1–25 in *Animal Models of Epilepsy: Methods and Innovations*, edited by S. C. Baraban. Humana Press, Totowa, NJ.

Lo Nigro, C., C. S. Chong, A. C. Smith, W. B. Dobyns, R. Carrozzo *et al.*, 1997 Point mutations and an intragenic deletion in *LIS1*, the lissencephaly causative gene in isolated lissencephaly sequence and Miller-Dieker syndrome. Hum. Mol. Genet. **6:** 157–164.

Lu, J., Q. Sun, X. Chen, H. Wang, Y. Hu *et al.*, 2005 Identification of dynein light chain 2 as an interaction partner of p21-activated kinase 1. Biochem. Biophys. Res. Commun. **331:** 153–158.

Lucanic, M., M. Kiley, N. Ashcroft, N. L'Etoile and H. J. Cheng, 2006 The *Caenorhabditis elegans* P21-activated kinases are differentially required for UNC-6/netrin-mediated commissural motor axon guidance. Development **133:** 4549–4559.

Lundquist, E. A., P. W. Reddien, E. Hartwieg, H. R. Horvitz and C. I. Bargmann, 2001 Three *C. elegans* Rac proteins and several alternative Rac regulators control axon guidance, cell migration, and apoptotic cell phagocytosis. Development **128:** 4475–4488.

McEwen, J. M., J. M. Madison, M. Dybbs and J. M. Kaplan, 2006 Antagonistic regulation of synaptic vesicle priming by Tomosyn and UNC-13. Neuron **51:** 303–315.

McIntire, S. L., E. Jorgensen and H. R. Horvitz, 1993 Genes required for GABA function in *Caenorhabditis elegans*. Nature **364:** 334–337.

McMullan, R., E. Hiley, P. Morrison and S. J. Nurrish, 2006 Rho is a presynaptic activator of neurotransmitter release at pre-existing synapses in C. elegans. Genes. Dev. **20:** 65–76.

Menzel, N., A. Chari, U. Fischer, M. Linder and T. Raabe, 2007 A 5′-fluorosulfonylbenzoyladenosine-based method to identify physiological substrates of a *Drosophila* p21-activated kinase. Anal. Biochem. **368:** 178–184.

Miller, K. G., A. Alfonso, M. Nguyen, J. A. Crowell, C. D. Johnson *et al.*, 1996 A genetic selection for *Caenorhabditis elegans* synaptic transmission mutants. Proc. Natl. Acad. Sci. USA **93:** 12593–12598.

Nguyen, M., A. Alfonso, C. D. Johnson and J. B. Rand, 1995 *Caenorhabditis elegans* mutants resistant to inhibitors of acetylcholinesterase. Genetics **140:** 527–535.

Nonet, M. L., J. E. Staunton, M. P. Kilgard, T. Fergestad, E. Hartwieg *et al.*, 1997 *Caenorhabditis elegans rab-3* mutant synapses exhibit impaired function and are partially depleted of vesicles. J. Neurosci. **17:** 8061–8073.

Nonet, M. L., O. Saifee, H. Zhao, J. B. Rand and L. Wei, 1998 Synaptic transmission deficits in *Caenorhabditis elegans* synaptobrevin mutants. J. Neurosci. **18:** 70–80.

Patel, L. S., H. J. Wenzel and P. A. Schwartzkroin, 2004 Physiological and morphological characterization of dentate granule cells in the *p35* knock-out mouse hippocampus: evidence for an epileptic circuit. J. Neurosci. **24:** 9005–9014.

Pavlidis, P., M. Ramaswami and M. A. Tanouye, 1994 The *Drosophila easily shocked* gene: a mutation in a phospholipids synthetic pathway causes seizure, neuronal failure, and paralysis. Cell **79:** 23–33.

Pinkstaff, J. K., G. Lynch and C. M. Gall, 1998 Localization and seizure-regulation of integrin beta 1 mRNA in adult rat brain. Brain Res. Mol. Brain Res. **55:** 265–276.

Poinat, P., A. De Arcangelis, S. Sookhareea, X. Zhu, E. M. Hedgecock *et al.*, 2002 A conserved interaction between beta1 integrin/PAT-3 and Nck-interacting kinase/MIG-15 that mediates commissural axon navigation in *C. elegans*. Curr. Biol. **12:** 622–631.

Rankin, C. H., and S. R. Wicks, 2000 Mutations of the *Caenorhabditis elegans* brain-specific inorganic phosphate transporter *eat-4* affect habituation of the tap-withdrawal response without affecting the response itself. J. Neurosci. **20:** 4337–4344.

Rehberg, M., J. Kleylein-Sohn, J. Faix, T. H. Ho, I. Schulz *et al.*, 2005 *Dictyostelium* LIS1 is a centrosomal protein required for microtubule/cell cortex interactions, nucleus/centrosome linkage, and actin dynamics. Mol. Biol. Cell **16:** 2759–2771.

Richmond, J. E., and E. M. Jorgensen, 1999 One GABA and two acetylcholine receptors function at the *C. elegans* neuromuscular junction. Nat. Neurosci. **2:** 791–797.

Robatzek, M., and J. H. Thomas, 2000 Calcium/calmodulin-dependent protein kinase II regulates *Caenorhabditis elegans* locomotion in concert with a G(o)/G(q) signaling network. Genetics **156:** 1069–1082.

Sakamoto, R., D. T. Byrd, H. M. Brown, N. Hisamoto, K. Matsumoto *et al.*, 2005 The *Caenorhabditis elegans* UNC-14 RUN domain protein binds to the kinesin-1 and UNC-16 complex and regulates synaptic vesicle localization. Mol. Biol. Cell **16:** 483–496.

Schuske, K., A. A. Beg and E. M. Jorgensen, 2004 The GABA nervous system in *C. elegans*. Trends Neurosci. **27:** 407–414.

Shakir, M. A., J. S. Gill and E. A. Lundquist, 2006 Interactions of UNC-34 Enabled with Rac GTPases and the NIK kinase MIG-15 in *Caenorhabditis elegans* axon pathfinding and neuronal migration. Genetics **172:** 893–913.

Steven, R., T. J. Kubiseski, H. Zheng, S. Kulkami, J. Mancillas *et al.*, 1998 UNC-73 activates the Rac GTPase and is required for cell and growth cone migrations in *C. elegans*. Cell **92:** 785–795.

Steven, R., L. Zhang, J. Culotti and T. Pawson, 2005 The UNC-73/Trio RhoGEF-2 domain is required in separate isoforms for the regulation of pharynx pumping and normal neurotransmission in *C. elegans*. Genes Dev. **19:** 2016–2029.

Struckhoff, E. C., and E. A. Lundquist, 2003 The actin-binding protein UNC-115 is an effector of Rac signaling during axon pathfinding in *C. elegans*. Development **130:** 693–704.

Sulston, J., M. Dew and S. Brenner, 1975 Dopaminergic neurons in the nematode *Caenorhabditis elegans*. J. Comp. Neurol. **163:** 215–226.

Tischler, J., B. Lehner, N. Chen and A. G. Fraser, 2006 Combinatorial RNA interference in *Caenorhabditis elegans* reveals that redundancy between gene duplicates can be maintained for more than 80 million years of evolution. Genome Biol. **7:** R69.

Vashlishan, A. B., J. M. Madison, M. Dybbs, J. Bai, D. Sieburth *et al.*, 2008 An RNAi screen identifies genes that regulate GABA synapses. Neuron **58:** 346–361.

Wenzel, H. J., C. A. Robbins, L. H. Tsai and P. A. Schwartzkroin, 2001 Abnormal morphological and functional organization of the hippocampus in a *p35* mutant model of cortical dysplasia associated with spontaneous seizures. J. Neurosci. **21:** 983–998.

Williams, S. L., S. Lutz, N. K. Charlie, C. Vettel, M. Ailion *et al.*, 2007 Trio's Rho-specific GEF domain is the missing Galpha q effector in *C. elegans*. Genes Dev. **21:** 2731–2746.

Williams, S. N., C. J. Locke, A. L. Braden, K. A. Caldwell and G. A. Caldwell, 2004 Epileptic-like convulsions associated with LIS-1 in the cytoskeletal control of neurotransmitter signaling in *Caenorhabditis elegans*. Hum. Mol. Genet. **13:** 2043–2059.

Wu, Y. C., T. W. Cheng, M. C. Lee and N. Y. Weng, 2002 Distinct rac activation pathways control *Caenorhabditis elegans* cell migration and axon outgrowth. Dev. Biol. **250:** 145–155.

Xu, J., and C. E. Clancy, 2008 Ionic mechanisms of endogenous bursting in CA3 hippocampal pyramidal neurons: a model study. PLoS ONE **3:** e2056.

Yang, Y., J. Lu, J. Rovnak, S. L. Quackenbush and E. A. Lundquist, 2006 SWAN-1, a *Caenorhabditis elegans* WD repeat protein of the AN11 family, is a negative regulator of Rac GTPase function. Genetics **174:** 1917–1932.

Zipkin, I. D., R. M. Kindt and C. J. Kenyon, 1997 Role of a new Rho family member in cell migration and axon guidance in *C. elegans*. Cell **90:** 883–894.

Communicating editor: K. Kemphues

GENETICS

Supporting Information
http://www.genetics.org/cgi/content/full/genetics.109.106880/DC1

Pharmacogenetic Analysis Reveals a Post-Developmental Role for Rac GTPases in *Caenorhabditis elegans* GABAergic Neurotransmission

Cody J. Locke, Bwarenaba B. Kautu, Kalen P. Berry, S. Kyle Lee, Kim A. Caldwell and Guy A. Caldwell

DOI: 10.1534/genetics.109.106880

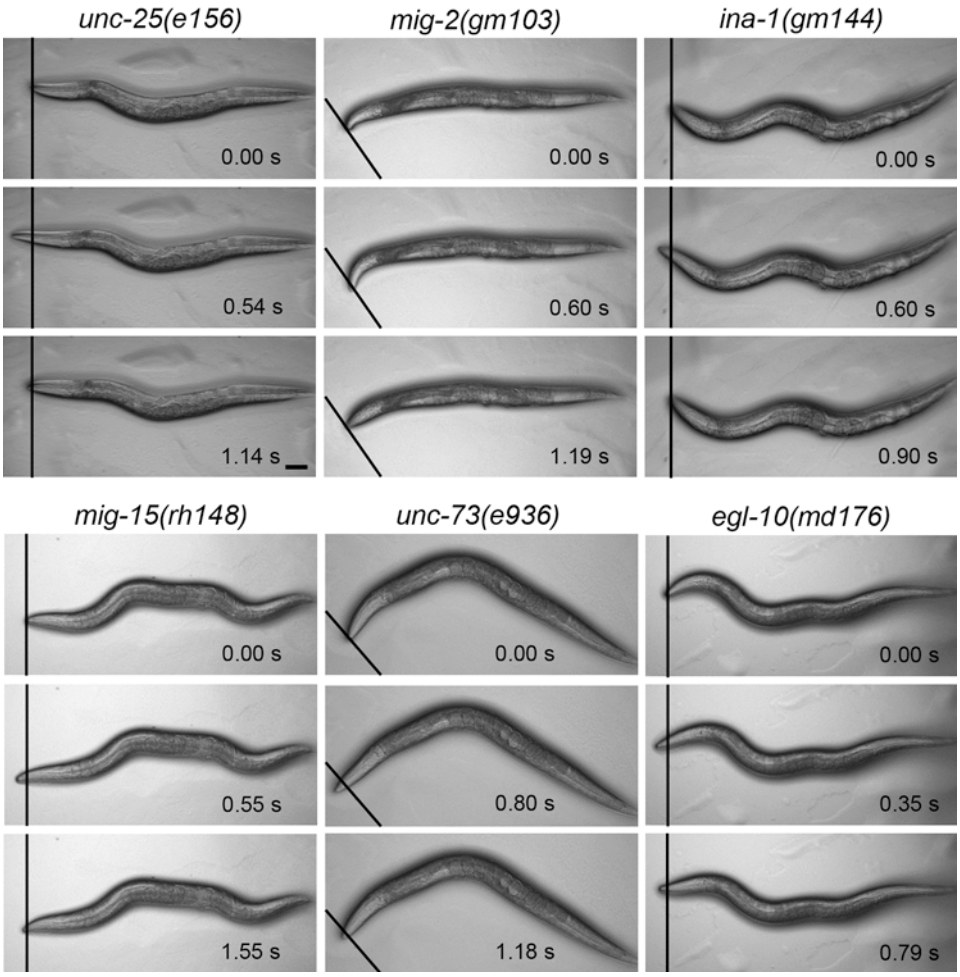

FIGURE S1.—Still frame images demonstrating *C. elegans* mutant strains with anterior convulsions in response to PTZ. The still images are representative frames from movies (25 frames per second), which are available in Supplementary Material. The black lines represent stationary reference points for visualization of anterior movements in relation to time (indicated in *s*). Anterior is to the left in all images, where lines are placed perpendicular to the original position of each worm's nose. The convulsions of a GABA mutant, *unc-25(e156)*, mimic those of a Rac gain-of-function mutant, *mig-2(gm103)*, and the Rac regulator mutants, *ina-1(gm144)*, *mig-15(rh148)*, and *unc-73(e936)*. A G protein signaling mutant, *egl-10(md176)*, which is deficient in general neurotransmitter release, also exhibits anterior convulsions on PTZ. Bar = 100 mm.

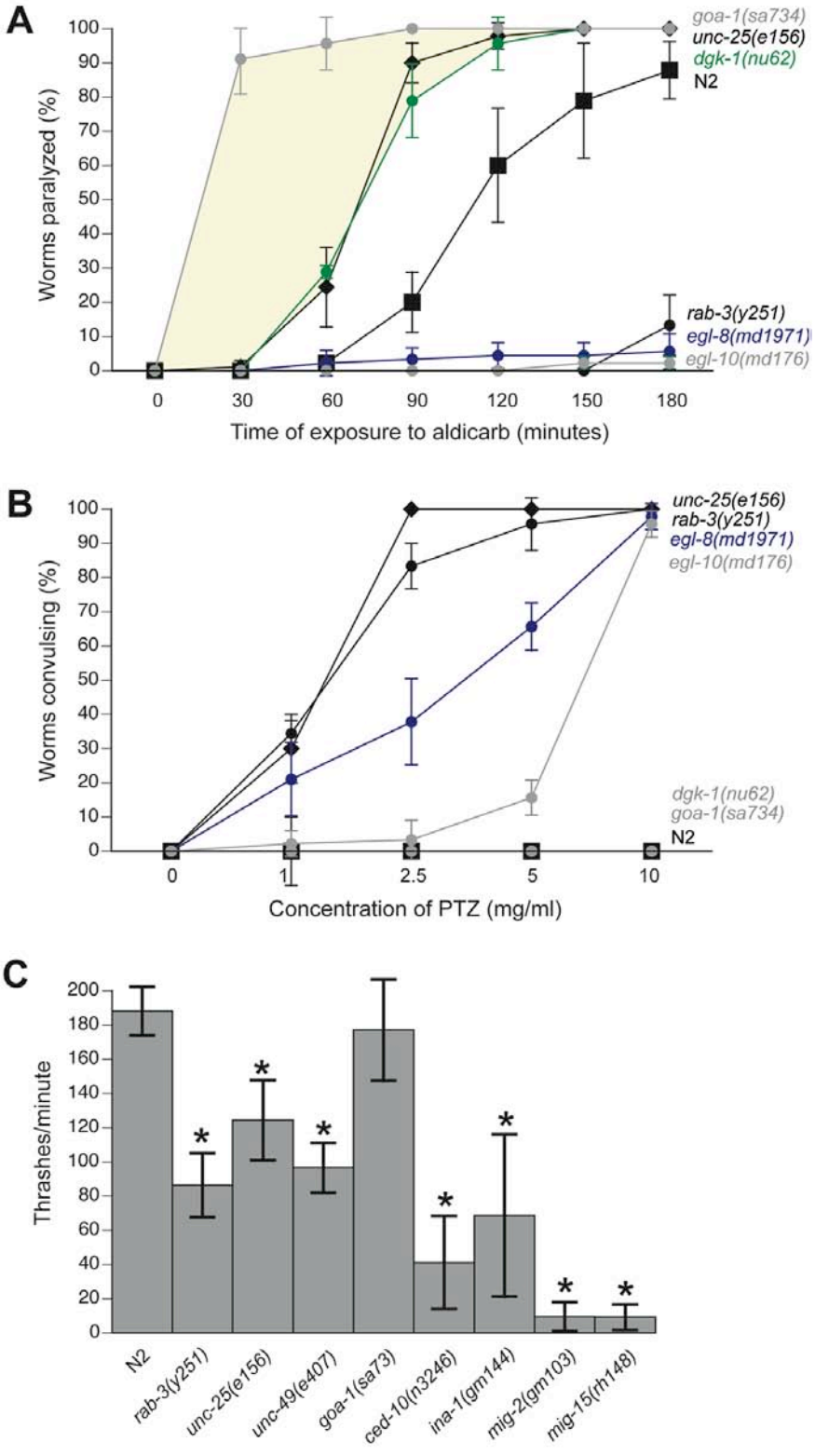

FIGURE S2.—Results from pharmacological and behavioral assays are inconsistent with a role for Rac GTPases and Rac regulators in heterotrimeric G protein signaling. (A-B) The response level (percent young adult worms paralyzed per total sample size; n=30 for each of three independent experiments) of various *C. elegans* strains is depicted for each 30-min. time point in three hours of exposure to 0.5 mM aldicarb (A) and each PTZ concentration, ranging from 0 to 10 mg/ml (B). Results from control

strains (shown collectively in black) are repeated from Figure 1 (B) and Figure 3 (A) for convenience. (A) Paralysis of a predicted null *goa-1* mutant, *sa734* (dark gray circles), which fails to inhibit excitatory cholinergic transmission at *C. elegans* neuromuscular junctions, was greatest. Similar aldicarb sensitivity was also observed for *dgk-1(nu62)* lf mutants (green circles), which are also characterized by excess levels of excitatory acetylcholine (ACh) transmission, as well as a strong GABA mutant, *unc-25(e156)* (black diamonds). Conversely, lf mutants for genes, which antagonize signaling through *goa-1* and *dgk-1*, exhibited resistance to aldicarb (blue and light gray circles); these mutants demonstrated similar aldicarb sensitivities as *rab-3(y251)* mutants (black circles), which are deficient in general synaptic transmission. Trends in aldicarb sensitivity are shown with pale yellow shading. (B) Despite similar sensitivities to aldicarb as a representative GABA mutant, *goa-1(sa734)* and *dgk-1(nu62)* mutants (collectively shown by light gray circles) did not exhibit PTZ-induced anterior convulsions, like *unc-25(e156)* (black diamonds) and *rab-3(y251)* (black circles). However, *egl-8(md1971)* (blue circles) and *egl-10(md176)* (dark gray circles) did exhibit PTZ-induced anterior convulsions. Each data point represents mean ± mean of standard deviations. Each data point represents mean ± standard deviation. (C) The number of thrashes per minute for one-day old adult worms (n=30) are shown. A mutant with excess ACh transmission, *goa-1(sa734)*, thrashes at a wild type (WT) rate. Yet, Rac signaling pathway mutants, including *ced-10(n3246)*, *mig-2(gm103)*, *ina-1(gm144)*, and *mig-15(rh148)* mutants, like a representative general synaptic transmission, *rab-3(y251)*, and GABA, *unc-25(e156)*, mutants, thrash at significantly slower rates than N2 WT worms. Each data point represents mean ± standard deviation. *$p < 0.05$; Student's t-test.

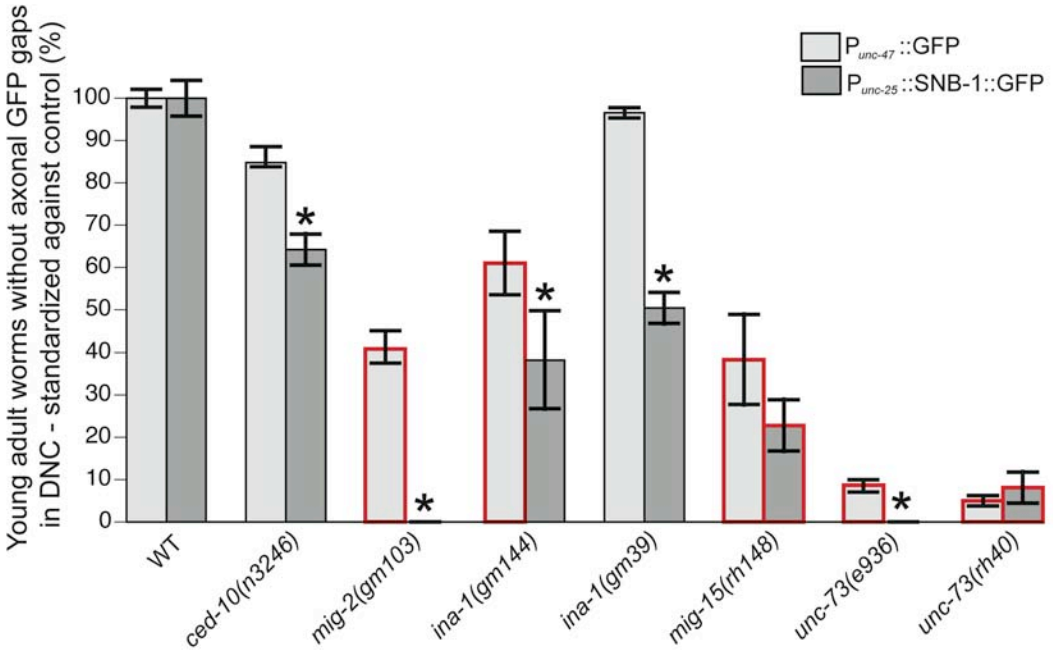

FIGURE S3.—Rac GTPase and canonical Rac regulator mutants exhibit synaptic vesicle misaccumulations and some architectural breaks in GABAergic DD motor neurons. The percentage of axonal GFP gaps (percent worms with gaps per total sample size; n=30 for each of three independent experiments) in GABAergic D-type motor neurons of dorsal nerve cords (DNCs) of young adult hermaphrodites in various *C. elegans* strains is depicted. Soluble GFP expression showed no significant architectural breaks in the DNC axons of wild type (WT), *ced-10(n3246)*, or *ina-1(gm39)* young adult *oxIs12* (P_{unc-47}::GFP) worms (light gray bars). However, *mig-2(gm103)*, *ina-1(gm144)*, *mig-15(rh148)*, *unc-73(e936)*, and *unc-73(rh40)* mutants had significant percentages of soluble GFP gaps in young adult GABAergic Dtype motor neurons of the DNC, indicating architectural abnormalities. GABAergic neuron-specific expression of a synaptobrevin-1 (SNB-1) and GFP translational fusion protein in young adult GABAergic D-type motor neurons revealed significant percentages of synaptic vesicle misaccumulations, as demonstrated by axonal SNB-1::GFP gaps, in all Rac signaling mutants tested (dark gray bars). Architectural defects in the DNCs of *mig-15(rh148)* and *unc-73(rh40)* mutants could not be separated from synaptic vesicle transport defects. Each data point represents mean ± mean of standard deviations. *$p < 0.05$; Fisher's Exact Test. Asterisks for P_{unc-25}::SNB-1::GFP data indicate significant differences in percentages of axonal GFP gaps, compared to the WT *juIs1* background and P_{unc-47}::GFP data for the same mutant, suggesting that synaptic vesicle transport defects (SNB-1::GFP gaps) occur independently of architectural defects (soluble GFP gaps). Red outlines around bars, which represent P_{unc-47}::GFP, indicate that percentages of axonal GFP gaps are significantly different from the WT *oxIs12* background. Red outlines around bars, which represent P_{unc-25}::SNB-1::GFP, indicate that percentages of axonal GFP gaps are significantly different from the WT *juIs1* background, but are not significantly different from an *oxIs12*-bearing Rac signaling pathway mutant, which carries the same allele. The *ced-10(n3246)* mutants with *juIs1* are heterozygous for the dominant *n3246* allele, while *ced-10(n3246)* mutants with *oxIs12* are homozygous for the dominant *n3246* allele.

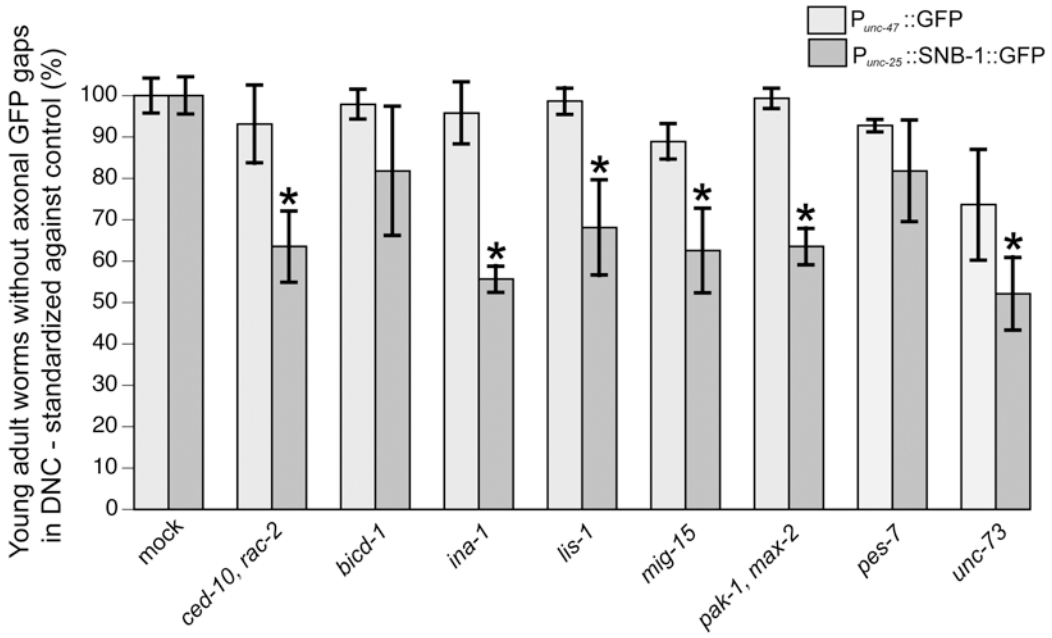

FIGURE S4.—Lactose-induced RNAi feeding against canonical Rac signaling pathway members results in synaptic vesicle misaccumulations, but not architectural breaks, in GABAergic D-type motor neurons of dorsal nerve cords. The percentage of axonal GFP gaps (percent young adult worms with gaps per total sample size; n=30 for each of three to five independent experiments) in GABAergic D-type motor neurons of dorsal nerve cords (DNCs) of various RNAi treatments is depicted. Soluble GFP expression showed no architectural breaks in the DNC axons of young adult *oxIs12* (P_{unc-47}::GFP) worms with mock (α-synuclein) RNAi or RNAi against Rac signaling pathway members (light gray bars). Yet, RNAi against most Rac signaling pathway members resulted in misaccumulated synaptic vesicles, as revealed by gaps in GABAergic neuron-specific expression of a synaptobrevin-1 (SNB-1) and GFP translational fusion protein (dark gray bars). Despite not significantly disrupting SNB-1::GFP localization in ventral nerve cords (VNCs) (see Figure 5) of young adults, *mig-15*(RNAi) yielded SNB-1::GFP misaccumulations in young adult DNCs. Conversely, *pes-7*(RNAi) did not significantly disrupt SNB-1::GFP localization in DNCs, despite affecting VNCs (see Figure 5). Combinatorial RNAi was used against two of three triply redundant Racs, *ced-10* and *rac-2*. Results from mock RNAi against *oxIs12* worms were used to standardize other results with *oxIs*12 worms. Likewise, results from mock RNAi against *juIs*1 (P_{unc-25}::SNB-1::GFP) worms were used to standardize other results with *juIs1* worms. Each data point represents mean ± mean of standard deviations. *$p < 0.05$; Fisher's Exact Test.

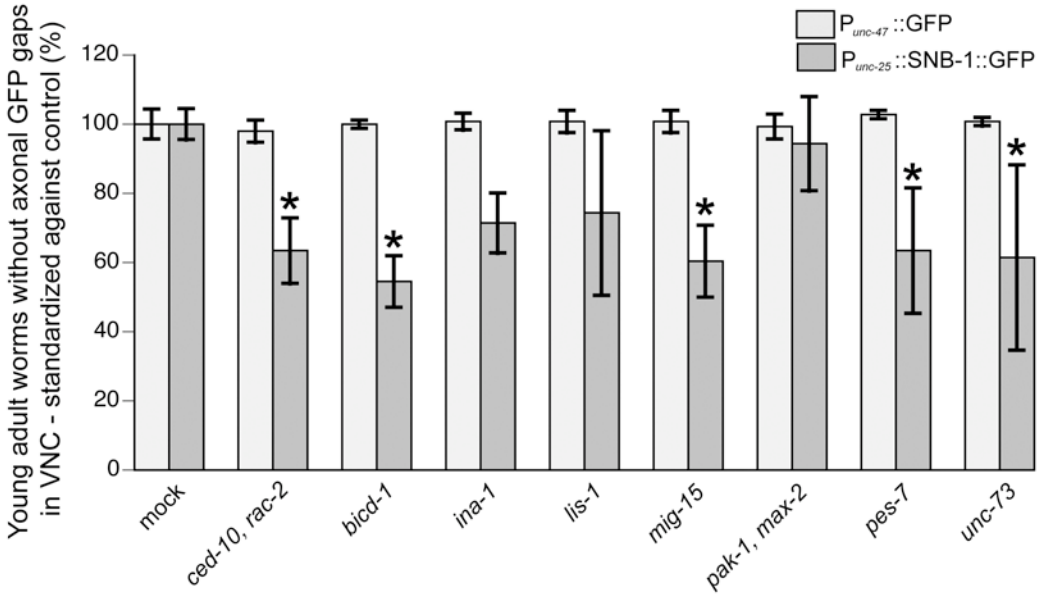

FIGURE S5.—Lactose-induced RNAi feeding in parental generations, instead of first generation progeny, further suggests a post-developmental role for a Rac signaling pathway in dynein-mediated GABAergic synaptic vesicle transport. The percentage of axonal GFP gaps (percent young adult worms with gaps per total sample size; n=30 for each of three independent experiments) in GABAergic D-type motor neurons of ventral nerve cords (VNCs) of various RNAi treatments is depicted. Soluble GFP expression showed no architectural breaks in the VNC axons of young adult *oxIs12* (P_{unc-47}::GFP) worms with mock (α-synuclein) RNAi or RNAi against Rac signaling pathway members (light gray bars). Yet, RNAi against Rac signaling pathway members, except for combinatorial RNAi against two PAK orthologs, *pak-1* and *max-2*, resulted in misaccumulated synaptic vesicles, as revealed by gaps in GABAergic neuron-specific expression of a synaptobrevin-1 (SNB-1) and GFP translational fusion protein (dark gray bars). Despite not significantly disrupting SNB-1::GFP localization in VNCs of young adults (see Figure 5), *mig-15*(RNAi) yielded SNB-1::GFP misaccumulations in VNCs of L1 larvae. Combinatorial RNAi was also used against two of three triply redundant Racs, *ced-10* and *rac-2*. Results from mock RNAi against *oxIs12* worms were used to standardize other results with *oxIs*12 worms. Likewise, results from mock RNAi against *juIs*1 (P_{unc-25}::SNB-1::GFP) worms were used to standardize other results with *juIs1* worms. Each data point represents mean ± mean of standard deviations. *$p < 0.05$; Fisher's Exact Test.

FILE S1

Supporting Methods and Materials

Rescue of *ina-1*:

An *ina-1* cDNA (*F54G8.3*) was made by RT-PCR from total N2 RNA samples. Primers used for *ina-1* cDNA isolation were Primer 1: 5' gg-gac-tac-aag-gac-gac-gat-gac-aag-atg-cgt-gaa-tgt-ata-att-agc 3' and Primer 2: 5' gg-cta-aag-tcc-cgt-atc-agc-cc 3'. A Gateway entry vector was generated by using Gateway recombination cloning (Invitrogen) to insert the *ina-1* cDNA into pDONR221 via BP reaction. The sequence verified *ina-1* cDNA was shuttled into a Gateway destination vector, pDEST-UNC-47, via an LR reaction. The pDEST-UNC-47 destination vector was generated by cloning an *unc-47* promoter (Williams *et al.* 2004) into pDEST-UNC-54 (Hamamichi *et al.* 2008) after removing the *unc-54* promoter at the *HindIII* and *KpnI* sites. Two independent transgenic (Tg) P_{unc-47}::*ina-1* lines were generated by microinjecting pDEST-UNC-47-*ina-1* and an intestinal GFP marker, P_{ges-1}::*gfp*, into wild type (N2) young adult hermaphrodites at a concentration of 100 ng/μL. Genetic crosses were done by first crossing N2 males to P_{unc-47}::*ina-1* hermaphrodites, verified by intestinal GFP expression. Tg male offspring were then crossed with hermaphrodites of target mutant strains. GFP-positive progeny from these crosses were tested for homozygosity of the target gene by uncoordination, PTZ-induced convulsions, and thrashing, consistent with homozygosity of non-Tg mutants.

Fluorescence Microscopy:

To observe possible alterations in GABAergic D-type motor neuron architecture, *oxIs12* males were crossed with hermaphrodites from strains carrying *ced-10(n3246)*, *ina-1(gm39)*, *ina-1(gm144)*, *mig-2(gm103)*, *mig-15(rh148)*, *unc-73(e936)*, or *unc-73(rh40)*. After homozygosing for *oxIs12* and a mutation of interest, young adult hermaphrodites were examined for proper axon pathfinding along the full lengths of the ventral and dorsal nerve cords, whereas L1 larvae hermaphrodites were examined for proper axon pathfinding along the full length of the ventral nerve cord (Knobel *et al.* 2001). Both *mig-2(gm103)* and *mig-15(rh148)* mutants with *oxIs12* were generated by meiotic recombination, as previously described (Poinat *et al.* 2002) and selected based upon uncoordination and hypersensitivity to aldicarb and/or PTZ.

To score synaptic vesicle distribution defects in GABAergic D-type motor neurons of mutant strains of interest, *juIs1* males were crossed with hermaphrodites from strains carrying *ced-10(n3246)*, *ina-1(gm39)*, *ina-1(gm144)*, *mig-2(gm103)*, *mig-15(rh148)*, *unc-73(e936)*, or *unc-73(rh40)*. After homozygosing for *juIs1* and a mutation of interest, except for *ced-10(n3246)*, young adult hermaphrodites were assayed for SNB-1::GFP accumulation along the full lengths of the ventral and dorsal nerve cords, whereas L1 larvae hermaphrodites were assayed for SNB-1::GFP accumulation along the full lengths of the ventral nerve cord. SNB-1::GFP misaccumulations associated with CED-10 were scored with *ced-10(n3246)* heterozygotes, due to a failure to isolate homozygotes with *juIs1* and dominance from *n3246* (Yang *et al.* 2006). Architectural defects and synaptic vesicle distribution defects were also examined, as previously described, following lactose-induced RNAi feeding against *oxIs12* and *juIs1*

hermaphrodites, respectively. The average ventral nerve cord gap sizes for young adult and L1 worms were obtained by capturing images with a Photometrics Cool Snap CCD camera driven by MetaMorph software (Universal Imaging). Ten images from ten worms of each strain were captured for analysis. Gaps in SNB-1::GFP expression were then measured with MetaMorph. For all fluorescence microscope assays, young adult hermaphrodites were mounted in 3 mM levamisole on 2% agarose pads and observed with a Nikon Eclipse E600 epifluorescence microscope with DIC optics and Endow GFP HYQ and UV-2E/C DAPI filter cubes (Chroma, Inc.). All analyses were made at 400X-600X magnification for young adult worms and 1000X magnification for L1 larvae.

RNA interference:

Lactose-induced RNA interference (RNAi) by bacterial feeding was performed as previously described (Locke *et al.* 2006), except that NGM with 0.25% lactose was used. RNAi feeding against hermaphroditic parents (supporting Figure 5), in addition to first generation offspring (Figure 5), was employed for fluorescence microscopy of young adult ventral nerve cords. The L4440 dsRNA production vectors for all RNAi experiments, except for α-synuclein (α-syn), a mock RNAi control, were obtained from a *C. elegans* RNAi library (MRC, Cambridge, UK) (Kamath *et al.* 2003). Experiments with α-syn (RNAi) were performed after Gateway recombination cloning of *α-syn* cDNA into a Gateway-converted L4440 plasmid. Primers used for α-syn cDNA production were Primer 1: 5' ggg-gac-aag-ttt-gta-caa-aaa-agc-agg-cta-cat-gga-cgt-gtt-cat-gaa-ggg-c 3' and Primer 2: 5' ggg-gac-cac-ttt-gta-caa-gaa-agc-tgg-gtg-tta-ggc-ttc-agg-ttc-gta-gtc-ttg 3'.

SUPPORTING REFERENCES

Hamamichi, S., R. N. Rivas, A. L. Knight, S. Cao, K. A. Caldwell, and G. A. Caldwell, 2008 Hypothesis-based RNAi screening identifies neuroprotective genes in a Parkinson's disease model. Proc. Natl. Acad. Sci. U S A **105:** 728-733.

Kamath, R. S., A. G. Fraser, Y. Dong, G. Poulin, R. Durbin *et al.*, 2003 Systematic functional analysis of the *Caenorhabditis elegans* genome using RNAi. Nature **421:** 231-237.

Knobel, K. M., W. S. Davis, E. M. Jorgensen, and M. J. Bastiani, 2001 UNC-119 suppresses axon branching in *C. elegans*. Development **128:** 4079-4092.

Locke, C. J., S. N. Williams, E. M. Schwarz, G. A. Caldwell, and K. A. Caldwell, 2006 Genetic interactions among cortical malformation genes that influence susceptibility to convulsions in *C. elegans*. Brain Res. **1120:** 23-34.

Poinat, P., A. De Arcangelis, S. Sookhareea, X. Zhu, E. M. Hedgecock *et al.*, 2002 A conserved interaction between beta1 integrin/PAT-3 and Nck-interacting kinase/MIG-15 that mediates commissural axon navigation in *C. elegans*. Curr. Biol. **12:** 622-631.

Yang, Y., J. Lu, J. Rovnak, S. L. Quackenbush, and E. A. Lundquist, 2006 SWAN-1, a *Caenorhabditis elegans* WD repeat protein of the AN11 family, is a negative regulator of Rac GTPase function. Genetics **174:** 1917-1932.

FILES S2-S10

Supporting Videos

Files S2-S10 are available for download as .mov files at http://www.genetics.org/cgi/content/full/genetics.109.106880/DC1.

File S2: Representative GABA mutant with anterior convulsions in response to 10 mg/ml PTZ. The strong mutant, *unc-25(e156)*, is deficient in GABA synthesis and displays PTZ-induced anterior convulsions. This movie is representative of the behavioral responses to PTZ from all GABA mutant strains upon exposure to PTZ.

File S3: Rac GTPase, *ced-10*, mutant with anterior convulsions in response to 10 mg/ml PTZ. The Rac gain-of-function mutant, *ced-10(n3246)*, exhibits PTZ-induced anterior convulsions. This behavioral response is reminiscent of GABA mutant convulsions.

File S4: Rac GTPase, *mig-2*, mutant with anterior convulsions in response to 10 mg/ml PTZ. The Rac gain-of-function mutant, *mig-2(gm103)*, exhibits PTZ-induced anterior convulsions. This behavioral response is reminiscent of GABA mutant convulsions.

File S5: Rac GTPase regulator mutant, *ina-1*, with anterior convulsions in response to 10 mg/ml PTZ. The Rac regulator mutant, *ina-1(gm39)*, is deficient in integrin activation and displays PTZ-induced anterior convulsions. This behavioral response mimics those of Rac gain-of-function and GABA mutants in the presence of PTZ.

File S6: Rac GTPase regulator mutant, *mig-15*, with anterior convulsions in response to 10 mg/ml PTZ. The Rac regulator mutant, *mig-15(rh80)*, is deficient in integrin-mediated kinase activity and displays PTZ-induced anterior convulsions. This behavioral response mimics those of Rac gain-of-function and GABA mutants in the presence of PTZ.

File S7: Rac GTPase regulator mutant, *unc-73*, with anterior convulsions in response to 10 mg/ml PTZ. The Rac regulator mutant, *unc-73(e936)*, fails to activate redundant Racs and demonstrates PTZ-induced anterior convulsions. This behavioral response is reminiscent of Rac gain-of-function and GABA mutant convulsions.

File S8: Representative general synaptic transmission mutant with anterior convulsions in response to 10 mg/ml PTZ. The mutant, *rab-3(y251)*, is deficient in synaptic vesicle targeting and, as a result, general synaptic transmission. This mutant exhibits PTZ-induced anterior convulsions that are reminiscent of Rac gain-of-function and GABA mutant convulsions. This movie is representative of the behavioral responses to PTZ from other general synaptic transmission mutant strains upon exposure to PTZ.

File S9: Triple glutamate-gated chloride channel mutant with anterior convulsions in response to 10 mg/ml PTZ. A triple glutamate-gated chloride channel mutant [*avr-14(ad1302); avr-15(ad1051) glc-1(pk54)*] is deficient in inhibitory glutamate transmission at the nerve ring and demonstrates PTZ-induced anterior convulsions. This behavioral response is reminiscent of Rac gain-of-function and GABA mutant convulsions, but is less frequent and intense.

File S10: Heterotrimeric G protein signaling mutant, *egl-10*, with anterior convulsions in response to 10 mg/ml PTZ. The heterotrimeric G protein signaling mutant, *egl-10(md176)*, is deficient in neurotransmitter release and demonstrates PTZ-induced anterior convulsions. This behavioral response is reminiscent of Rac gain-of-function and GABA mutant convulsions, despite conflicting responses to aldicarb.

TABLE S1

***C. elegans* SNB-1::GFP Axonal Gap Quantifications**

Gene name	Allele name	L1 interpunctal gap width (μm)	L1 gap number	Adult interpunctal gap width (μm)	Adult gap number
mig-2	*gm103*	9.7 ± 2.0	1.0 ± 0.0	28.2 ± 7.5	1.7 ± 0.7
ina-1	*gm144*	9.0 ± 1.9	1.3 ± 0.5	23.4 ± 11.7	1.7 ± 0.7
mig-15	*rh148*	10.1 ± 1.8	1.0 ± 0.0	25.2 ± 6.7	1.2 ± 0.4
unc-73	*e936*	8.8 ± 2.5	1.0 ± 0.0	31.3 ± 8.1	1.4 ± 0.7
unc-73	*rh40*	8.4 ± 2.0	1.0 ± 0.0	27.6 ± 8.4	1.3 ± 0.5